DOPPLER FREQUENCY ESTIMATION IN PULSE DOPPLER RADAR SYSTEMS

A THESIS

SUBMITTED TO THE DEPARTMENT OF ELECTRICAL AND

ELECTRONICS ENGINEERING

AND THE INSTITUTE OF ENGINEERING AND SCIENCES

OF BILKENT UNIVERSITY

IN PARTIAL FULFILLMENT OF THE REQUIREMENTS

FOR THE DEGREE OF

MASTER OF SCIENCE

By

Hamza Soğancı

August 2009

I certify that I have read this thesis and that in my opinion it is fully adequate, in scope and in quality, as a thesis for the degree of Master of Science.

Assist. Prof. Dr. Sinan Gezici (Supervisor)

I certify that I have read this thesis and that in my opinion it is fully adequate, in scope and in quality, as a thesis for the degree of Master of Science.

Prof. Dr. Orhan Arıkan

I certify that I have read this thesis and that in my opinion it is fully adequate, in scope and in quality, as a thesis for the degree of Master of Science.

Assist. Prof. Dr. İbrahim Körpeoğlu

Approved for the Institute of Engineering and Sciences:

Prof. Dr. Mehmet Baray
Director of Institute of Engineering and Sciences

ABSTRACT

DOPPLER FREQUENCY ESTIMATION IN PULSE DOPPLER RADAR SYSTEMS

Hamza Soğancı
M.S. in Electrical and Electronics Engineering
Supervisor: Assist. Prof. Dr. Sinan Gezici
August 2009

Pulse Doppler radar systems are one of the most common types of radar systems, especially in military applications. These radars are mainly designed to estimate two basic parameters of the targets, range and Doppler frequency. A common procedure of estimating those parameters is matched filtering, followed by pulse Doppler processing, and finally one of the several constant false alarm rate (CFAR) algorithms. However, because of the structure of the waveform obtained after pulse Doppler processing, CFAR algorithms cannot always find the Doppler frequency of a target accurately. In this thesis, two different algorithms, maximum selection and successive cancelation, are proposed and their performances are compared with the optimal maximum likelihood (ML) solution. These proposed algorithms both utilize the advantage of knowing the waveform structure of a point target obtained after pulse Doppler processing in the Doppler frequency domain. Maximum selection basically chooses the Doppler frequency cells with the largest amplitudes to be the ones where there is a target. On the other hand, successive cancelation is an iterative algorithm. In each iteration, it finds a target that minimizes a specific cost function, until there are no more

targets. The performances of these algorithms are investigated for several different point target scenarios. Moreover, the performances of the algorithms are tested on some realistic target models. Based on all those observations, it is concluded that maximum selection is a good choice for high SNR values when a low-complexity algorithm is needed, on the other hand, successive cancelation performs almost as well as the optimal solution at all SNR values.

Keywords: Pulse Doppler Radar, Doppler Frequency, Matched Filtering, Pulse Doppler Processing, CFAR, Maximum Likelihood.

ÖZET

DARBE DOPPLER RADAR SİSTEMLERİNDE DOPPLER FREKANSI KESTİRİMİ

Hamza Soğancı
Elektrik ve Elektronik Mühendisliği Bölümü Yüksek Lisans
Tez Yöneticisi: Yard. Doç. Dr. Sinan Gezici
Ağustos 2009

Darbe Doppler radar sistemleri özellikle askeri uygulamalarda sıkça kullanılan radar sistemlerinden biridir. Bu radarlar temelde hedeflerin iki önemli parametresi olan mesafe ve Doppler frekanslarını kestirmek için tasarlanmıştır. Bunu yapmanın en genel yolu, önce uyumlu filtreleme, sonra darbe Doppler işleme ve son olarak da pek çok farklı Sabit Yanlış Alarm Oranlı (SYAO) algoritmalardan birinin uygulanmasıdır. Ancak darbe Doppler işlemeden sonra elde edilen sinyal yapısı yüzünden, SYAO algoritmaları hedeflerin Doppler frekanslarını hassas bir şekilde kestiremezler. Bu tezde Maksimum Seçim ve Ardışık Çıkarma adıyla iki değişik algoritma önerildi ve bu algoritmaların performası optimal çözüm olan Maksimum Olabilirlik çözümüyle karşılaştırıldı. Önerilen bu algoritmaların her ikisi de nokta bir hedeften gelen sinyalin darbe Doppler işlemeden sonra elde edilen yapısının bilinmesi avantajını kullanmaktadır. Maksimum Seçim algoritması en yüksek değerli Doppler frekans hücrelerini hedeflerin bulunduğu hücreler olarak seçer. Ardışık Çıkarma algoritması ise tekrarlanan bir algoritmadır. Her tekrarda bir maliyet fonksiyonunun en küçük değerini veren bir hedef bulur ve bunu hiçbir hedef kalmayana kadar tekrar eder. Bu algoritmaların performansları pek çok değişik nokta hedef senaryosu için analiz edildi. Ayrıca bu algoritmaların

performansları bazı gerçekçi hedef modelleri üzerinde de test edildi. Bütün bu gözlemlerin sonucunda, Maksimum Seçim algoritmasının yüksek sinyal gürültü oranlarında (SGO) ve basit algoritmalara ihtiyaç duyulduğu durumlarda kullanılabileceği görüldü. Diğer taraftan, Ardışık Çıkarma algoritmasının bütün SGO değerlerinde optimal çözüme yakın bir performans gösterdiği saptandı.

Anahtar Kelimeler: Darbe Doppler Radarı, Doppler Frekansı, Uyumlu Filtreleme, Darbe Doppler İşleme, SYAO, Maksimum Olabilirlik.

ACKNOWLEDGMENTS

I would like to express my thanks and gratitude to my supervisor Asst. Prof. Dr. Sinan Gezici for his supervision, suggestions and invaluable encouragement throughout the development of this thesis. Not just as a researcher, but also as a person with all his qualities he has been a role model to me. Also, I would like to thank Prof. Dr. Orhan Arıkan for being very helpful to me with his experience on my thesis topic. In addition, I would like to extend my special thanks to Asst. Prof. Dr. İbrahim Körpeoğlu for his valuable comments and suggestions on the thesis, and to Dr. Fatma Çalışkan for sharing the realistic target models with me for the studies in Chapter 5.

I wish to thank to all my colleagues in EE-514, M. Burak Güldoğan, Y.Kemal Alp, Ahmet Güngör, Mert Pilancı, Onur Tan, Aykut Yıldız, Kaan Duman and Hülya Ağın, for creating a great working atmosphere. Also special thanks to all my friends, the staff and the teachers in our department, who make it one of the bests.

Finally, my deepest gratitude goes to my family. My father, Hüseyin, my mother, Mukaddes, my sister, Mine, my brother, Murat, my brother in law, Cemil, my sister in law, Cemile, and my sweet nephews Elif, Zeynep, Serdar and Serhat. Not just during my graduate studies but during all my life, they believed in me and helped me achieve my goals. Their support has always been invaluable.

Contents

List of Figures

Dedicated to my family

Chapter 1

INTRODUCTION

1.1 Objectives and Contributions of This Work

"*R*adio *D*etection *A*nd *R*anging", which is the acronym for the word *radar* actually implies the function of a radar. All Radars are typically designed to detect targets and to find their ranges. Pulse Doppler radars, which is a special type of radar, are designed to not only provide range estimates but also to provide Doppler velocities of the detected targets. The Doppler velocity is the radial velocity of the detected target and hence provides important information for both the classification and the tracking of the detected targets.

Using a multi pulsed waveform facilitates the estimation of the Doppler frequency. The reflection after each pulse comes with the same delay basically, which determines the range of the targets, but the spectral analysis of each pulse's corresponding range bin gives the Doppler frequency of the target at that range [1].

A general detection procedure of pulse Doppler radars consists of three steps. The first step of this procedure is matched filtering. It is known that matched

filters are the receivers that maximizes the signal-to-noise ratio (SNR) [2]. In the second step, pulse Doppler processing is performed, which is simply taking the discrete Fourier transform (DFT) of the same range bins of each pulse. After these two steps, a detection matrix is obtained. Each element of this matrix corresponds to a specific range and Doppler frequency pair. At the final step, each of these elements is tested to determine whether there is a target at that specific range and Doppler frequency pair. This test is generally performed by using one of the several different constant false alarm rate (CFAR) algorithms. After pulse Doppler processing, the observed waveform in the Doppler domain has a sinc shape with high side lobes [1]. These high side lobes cause the CFAR algorithms to make mistakes, and also they can be detected as targets. Therefore, the Doppler frequency of the target at that range may not be found. The most common solution to this problem is windowing the data before pulse Doppler processing. But this solution comes with its own problems. Even though windowing reduces the side lobes, it also reduces the main lobe, which decreases the detection performance of the CFAR algorithms. Also, windowing causes an increase in the main lobe width, which decreases the accuracy of Doppler frequency estimation [3]. Therefore, using these traditional algorithms, it is very difficult to perform effective Doppler frequency estimation.

The waveform obtained after the pulse Doppler processing in the Doppler domain is well-known for a point target except the amplitude of the received signal and the Doppler frequency caused by the velocity of the target. In this thesis, we propose solutions based on this known waveform structure. Since the waveform is known except for some of its parameters and the noise is modeled as Gaussian, the optimal solution can be obtained as the maximum likelihood (ML) estimator [2], [4]. Since the optimal solution is very complex, we also propose two suboptimal solutions. The first one is *successive cancelation*, which finds the Doppler frequencies of the targets one by one in an iterative manner. In each iteration, it finds one target that minimizes a cost function and then recreates

the signal coming from that target and subtracts it from the received signal. It repeats doing this until there are no more targets. The second algorithm is called *maximum selection*, which simply uses the fact that the known waveform for a point target achieves its maximum at the Doppler frequency of the target; hence, it chooses the Doppler frequency bins with the largest amplitudes to be the ones where there is a target. Both of these solutions yield promising results. Maximum selection is an algorithm with very low complexity. At high SNR values, it performs very close to the optimal solution. Successive cancelation is a more complex algorithm but it performs almost as well as the optimal solution at all SNR values. These algorithms use the waveform model for a point target. However, they can still have reasonable performance for real targets, as investigated in Chapter 5.

1.2 Organization of the Thesis

The organization of the thesis is as follows. In Chapter 2, basics of target detection in pulse Doppler radars are presented. First, general radar waveforms are explained and then signal processing steps for pulse Doppler radars are discussed. Finally, some CFAR detection algorithms are explained in detail.

In Chapter 3, the reasons that make the Doppler frequency estimation difficult for traditional CFAR algorithms are listed. Then, the optimal solution for the estimation of the Doppler frequency of a point target is obtained. Finally, two suboptimal solutions, namely, successive cancelation and maximum selection, are proposed.

Simulation results for five different scenarios of point targets are provided in Chapter 4. For each of these scenarios, the performances of the optimal solution, successive cancelation and maximum selection are compared.

In Chapter 5, some realistic target models are given and the performance of the proposed algorithms are tested on those realistic target models.

Finally, Chapter 6 concludes the thesis by highlighting the main contributions and listing possible topics for future research.

Chapter 2

BASICS OF TARGET DETECTION IN PULSE DOPPLER RADAR SYSTEMS

In this chapter, radar waveforms are briefly introduced first. Then, basics of matched filtering and pulse Doppler processing, which are the most common procedures for processing pulse burst waveforms, are explained. Finally, fundamentals of target detection and constant false alarm rate (CFAR) detection algorithms are studied.

2.1 Radar Waveforms

A generic radar waveform can be modeled as

$$\tilde{x}(t) = a(t)\, e^{j[\Omega t + \theta(t)]} \tag{2.1}$$

where Ω is the radio frequency (RF) carrier frequency, $a(t)$ is the amplitude modulation of the RF carrier, and $\theta(t)$ is the phase or frequency modulation of

the carrier [1]. The complex envelope of this waveform can be written as

$$x(t) = a(t)\, e^{j\theta(t)} \ . \tag{2.2}$$

Radar waveforms can be categorized according to the two variables, $a(t)$ and $\theta(t)$, in equation (2.2). The amplitude modulating signal $a(t)$ determines whether the waveform is continuous or pulsed.For continuous wave (CW) waveforms, $a(t)$ is a constant, hence $x(t)$ in equation (2.2) is in the form of a complex exponential. For single pulse waveforms, $a(t)$ is a pulse with a finite support; that is, signal $x(t)$ is nonzero only for the duration of the pulse. For pulse burst waveforms, $a(t)$ is the sum of shifted pulses. Various types of radar waveforms are illustrated in Figure 2.1.

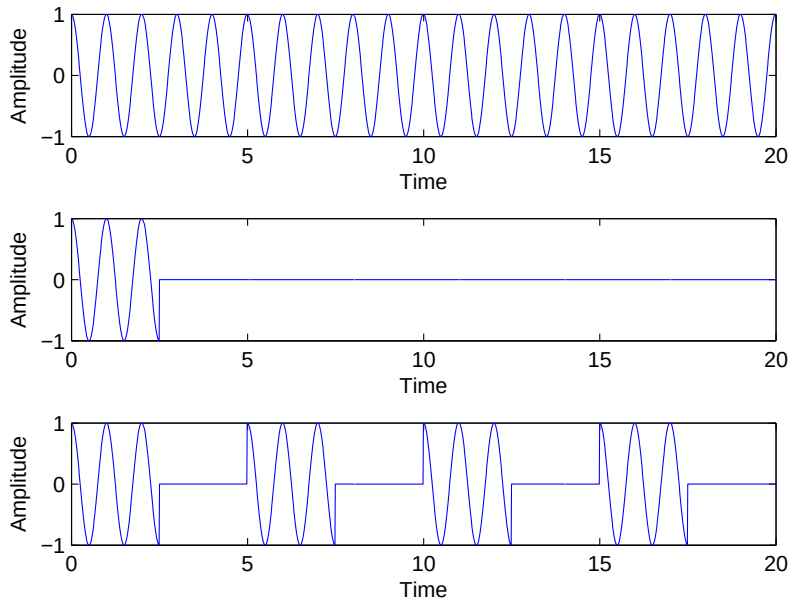

Figure 2.1: a) CW waveform. b) Single pulse waveform. c) Pulse burst waveform.

Most of the radar systems achieve transmission and reception with the same antenna. For such systems, pulsed waveforms are preferred as they facilitate time multiplexing of transmission and reception at a single antenna. In that case, the transmission is performed when $a(t)$ is non-zero, and the radar gets into reception mode when $a(t)$ is zero. To achieve better Doppler resolution,

pulse burst waveforms are used [1]-[8]. For single pulse waveforms, it is not possible to obtain any Doppler resolution at all.

The radar waveforms can also be categorized according to $\theta(t)$. There are significant variations according to the characteristics of $\theta(t)$. For example, the waveform can be frequency modulated, and in general the modulation can be linear or nonlinear. Phase modulation can also be used, which can be biphase or polyphase. In addition, there can be no phase or frequency modulation at all (cf. Figure 2.2).

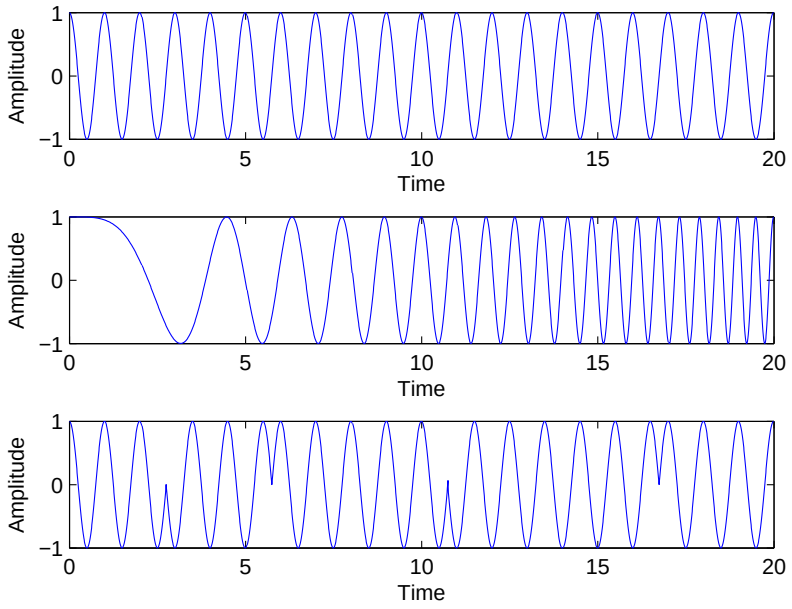

Figure 2.2: a) Waveform with no modulation. b) Frequency modulated waveform. c) Phase modulated waveform.

The main reason for applying frequency or phase modulation in radar waveforms is to achieve a better range resolution [1]-[8]. Without using these modulations, the range resolution is limited to the duration of the transmitted pulses. But due to concerns of energy and bandwidth, pulse durations cannot be smaller than certain limits.

2.2 Matched Filtering and Pulse Doppler Processing

In order to achieve better detection performance, it is desired to have a higher signal-to-noise ratio (SNR). Thus, it is important to have a receiver that maximizes the SNR. When the interference is modeled as white noise, the maximum SNR is achieved with the well-known matched filter. For a transmitted waveform $x(t)$, the corresponding matched filter is given by

$$h(t) = x^*(T_M - t) \ , \tag{2.3}$$

where $x^*(t)$ denotes the complex conjugate of $x(t)$, and T_M is the time instant at which the SNR is maximized.

In this case, the output of the matched filter is the result of the following convolution:

$$y(t) = \int_{-\infty}^{\infty} r(s)h(t-s)ds = \int_{-\infty}^{\infty} r(s)x^*(s + T_M - t)ds \ , \tag{2.4}$$

where $r(t)$ is the received signal. From equation (2.4), it is observed that the matched filter is actually a correlator that uses the transmitted waveform as the reference signal. Therefore, the output of the matched filter is a replica of the autocorrelation function of the transmitted waveform [1].

In the previous section, it was mentioned that frequency or phase modulated waveforms are used to achieve better range resolution. This is due to the fact that these waveforms have narrower autocorrelation functions than the waveforms without any frequency or phase modulation [1]-[8].

The matched filter uses the whole transmitted waveform as the reference signal. For pulse burst waveforms, the implementation of the matched filter can be easily performed since it is enough to use only one pulse as the reference signal

[1]. As it can be seen in Figure 2.3, the reflection signals after each transmitted pulse is matched filtered with just one transmitted pulse.

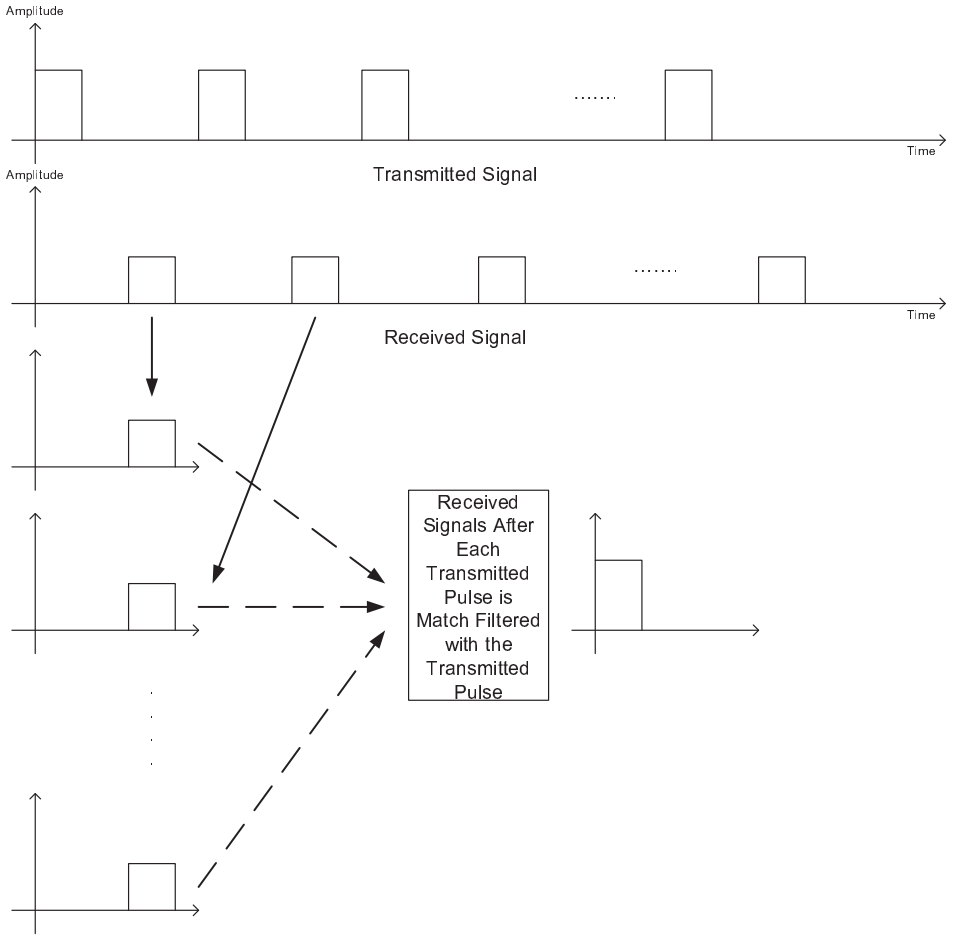

Figure 2.3: Match filtering process for pulse burst waveforms.

After this filtering operation, an $M \times N$ matrix is obtained, where M is the number of pulses and N is the number of samples collected between the transmission of consecutive pulses. This matrix will be used in pulse Doppler processing.

The pulse Doppler processing is a technique for the spectral analysis of each of the N columns of the matrix obtained after matched filtering [1]-[8]. Each of these N columns corresponds to a delay (equivalently, range). For each of these range bins, pulse Doppler processing makes an explicit spectral analysis, commonly using the discrete Fourier transform (DFT). After this spectral analysis, the

resulting matrix becomes the input for a target detection unit. N bins in each row of this new matrix correspond to range values, whereas M bins in each column correspond to Doppler frequencies (velocities). The pulse Doppler processing can be summarized as in Figure 2.4.

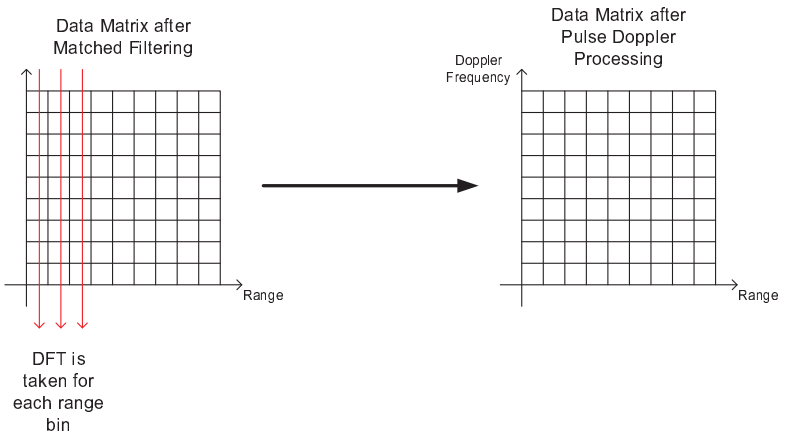

Figure 2.4: Pulse Doppler processing.

In the previous section, it was mentioned that pulse burst waveforms are used to improve the Doppler resolution. This is due to the fact that taking the DFT of each column yields a spectrum that is periodic with a period of the pulse repetition frequency (PRF) [1]-[8]. No matter what the number of pulses is, the spectrum is always periodic with this same period. Therefore, if there are more rows in the detection matrix, which corresponds to a larger number of pulses in the waveform, the principal period of this spectrum will be sampled with more points. As a result, if the same interval is sampled with more points, then the Doppler resolution will be higher.

2.3 Target Detection and CFAR Algorithms

After matched filtering and pulse Doppler processing, the received signal takes a form which is ready for target detection. As explained in the previous section,

after these processes an $M \times N$ matrix is obtained. Each element of this matrix corresponds to a specific range and Doppler frequency pair. Each of these elements is a candidate for possible targets. Using statistical hypothesis testing, a decision is made for each of these elements, stating whether there is a target at that range and Doppler frequency or not [2], [4].

Most of the common detection algorithms employ the observed signal to obtain a threshold for the hypothesis testing of each of the elements in the detection matrix. For the case in which the statistical distribution of the observed signal is known, it is possible to choose the threshold such that the false alarm rate of the hypothesis testing is constant. These algorithms are generally known as CFAR detection algorithms. But in real life applications, the statistical distribution of the observed signal is not known exactly. It is possible that the observed signal consists of pure noise and clutter, or there can be a target in the environment and the observed signal consists of noise, clutter and target. In such cases it is necessary to estimate the power of noise and clutter, and to use that information for setting the threshold [1]-[14].

There are various versions of CFAR algorithms, each of which has a different way of estimating the power of noise and clutter. Basically, each of those algorithms employs some of the cells in the detection matrix to obtain a threshold for each and every cell in this matrix. After finding the threshold for each cell, a decision is made for that cell. This procedure can be summarized as in Figure 2.5.

Different versions of CFAR algorithms differ basically in the choice of the reference cells. One of the most common and basic types of CFAR algorithms is cell averaging CFAR (CA-CFAR). This algorithm uses all the reference cells as in Figure 2.5 to estimate the interference (noise+clutter) power. Using these reference cells, an average for the interference power at the test cell is found. Based on this average, a threshold is determined to make the false alarm rate

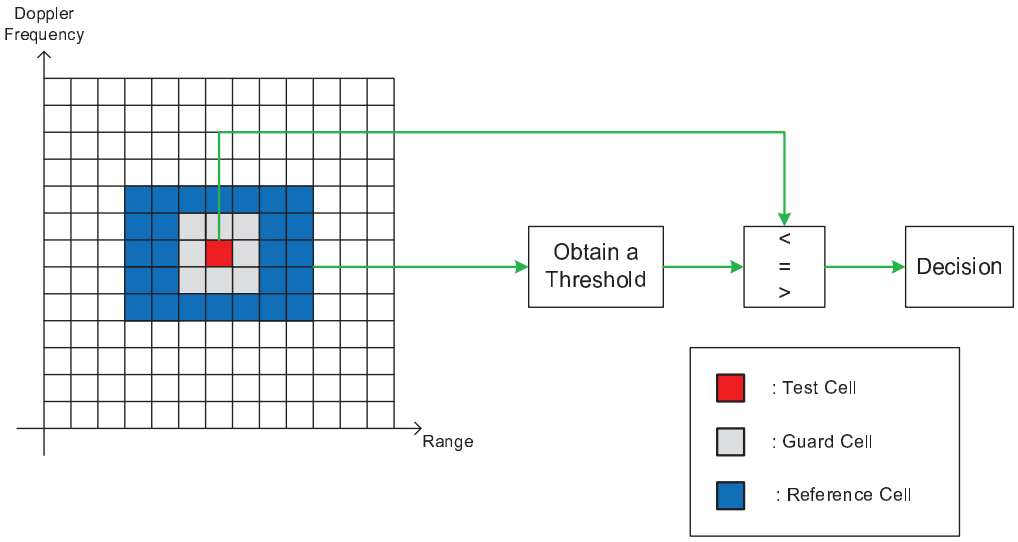

Figure 2.5: General CFAR algorithm.

constant, and the decision is made according to that threshold [1]-[15]. All the CFAR algorithms assume a basic distribution for the interference. For CA-CFAR, the most common distributions are Gaussian and Weibull [16], [17].

For the cases in which all the reference cells are coming from a homogeneous set, CA-CFAR performs well. Otherwise this algorithm needs to be modified. For example, if there is another target in the reference cells, this causes the estimated interference power to be higher than it really is. As a result, a higher threshold is found, which may result in a miss detection. To solve this problem, the smallest of cell averaging CFAR (SOCA-CFAR) algorithm is used. In this algorithm, the reference cells are divided into two groups. Then, the group with the smallest average power is used to determine the threshold [1], [15].

Another case of heterogeneous reference cells is the one with clutter edges. When there is a clutter edge in the reference cells, SOCA-CFAR can produces many false alarms. Since SOCA-CFAR uses the reference cells with the smaller average, this may cause the threshold to be low and as a result clutter edges can be detected as targets. To solve this problem, another similar algorithm, the

greatest of cell averaging CFAR (GOCA-CFAR), is used. In this algorithm, again the reference cells are divided into two groups, but this time the group with the higher average power is used to determine the threshold. This algorithm reduces the false alarms caused by clutter edges. However, the main problem with this algorithm is that it is possible to miss detect two close targets as the threshold is determined by using the reference cells that contain the other target [1], [15].

Another algorithm to solve the problem of two close targets is the trimmed mean CFAR (TM-CFAR). This algorithm does not use a number of reference cells with the highest power. In this way, it avoids setting a high threshold because of another close target [1]. Another dynamic version of this algorithm is the variably trimmed mean CFAR (VTM-CFAR). In that algorithm, the number of reference cells that are used is not constant. Instead, the number of ignored reference cells is decided after a preprocessing [18]-[20].

Another CFAR algorithm that performs well in the cases of close targets and clutter edges is switching CFAR (S-CFAR). In this algorithm, in the first step, all the reference cells are compared to a threshold. After that, if the number of reference cells higher than this threshold is larger than a number, all the reference cells are used to find the threshold for the test cell. Otherwise, only the reference cells with power higher than the threshold are used [21].

The order statistics CFAR (OS-CFAR) is another algorithm, which performs well in the case of two close targets. In this algorithm, all the reference cells are sorted according to their powers. Then, the cell that corresponds to a specified order is chosen and the power of this cell is used as the interference power at the test cell [12], [15], [22].

In the case of heterogeneous interference at the reference cells, the adaptive CFAR (A-CFAR) can be employed. In this algorithm, a homogeneous group

of reference cells is found first. After that, only the cells that belong to the homogeneous group are used to determine the threshold [23]-[25].

Chapter 3

ESTIMATION OF TARGET DOPPLER FREQUENCY

In this chapter, the signal model of a point target in the Doppler domain is presented, and the difficulties for the CFAR algorithms to estimate the Doppler frequencies of targets are explained based on that signal model. In addition, the optimal solution for Doppler frequency estimation is obtained. Finally, two suboptimal solutions are studied: First one is called the maximum selection algorithm, which uses the cells with highest amplitudes to estimate the Doppler frequencies of the targets; the second one is successive cancelation, which tries to estimate the Doppler frequency of targets consecutively.

3.1 Signal Model of a Point Target in Doppler Domain

In order to understand the basics of Doppler frequency estimation, it is essential to write down the signal model of a point target at some specified range bin. First of all, after matched filtering, if the velocity of the target is such that the

there is no Doppler shift (i.e., no relative motion of the target with respect to the radar), the received signal at the target's range bin, which is known as slow time received signal, is a constant; that is,

$$y[m] = A \ , \qquad m = 0, 1, \ldots, M-1 \ , \tag{3.1}$$

where M is the number of pulses. The Fourier transform of this constant is

$$Y(f) = A\frac{\sin[\pi f MT]}{\sin[\pi fT]}e^{-j\pi(M-1)fT}, \quad f \ \in \ [-PRF/2, +PRF/2) \tag{3.2}$$

where T is the pulse repetition interval [1], [6], which is equal to $1/PRF$. If the velocity of the point target is such that there is a Doppler shift of f_D, the slow time received signal and its Fourier transform become

$$y[m] = Ae^{j2\pi f_D mT} \ , \qquad m = 0, 1, \ldots, M-1 \ , \tag{3.3}$$

$$Y(f - f_D) = A\frac{\sin[\pi(f - f_D)MT]}{\sin[\pi(f - f_D)T]}e^{-j\pi(M-1)(f-f_D)T}, \quad f \ \in \ [-PRF/2, +PRF/2). \tag{3.4}$$

This waveform creates two problems decreasing the performance of traditional CFAR algorithms. The first problem is the fact that this waveform has very strong side lobes, especially when the number of pulses is small. Most pulse Doppler radar systems transmit a signal with a number of pulses such as 16, 32, 64, 128. For example, the waveform in the Doppler domain for 32 pulses can be seen in Figure (3.1), where $A = 1$ and $f_D = 0$. The high side lobes of this waveform cause the CFAR algorithms to result in a lot of false alarms. Also, these side lobes make it very difficult to find the exact Doppler frequency of the target since most of the cells at the range of the target is detected as possible targets.

The most common solution to the side lobe problem is to window the slow time received signal. Windowing reduces the side lobes effectively but they also present new problems. Each window function has different characteristics but, in general, these windows cause a decrease in the peak amplitude and SNR, which

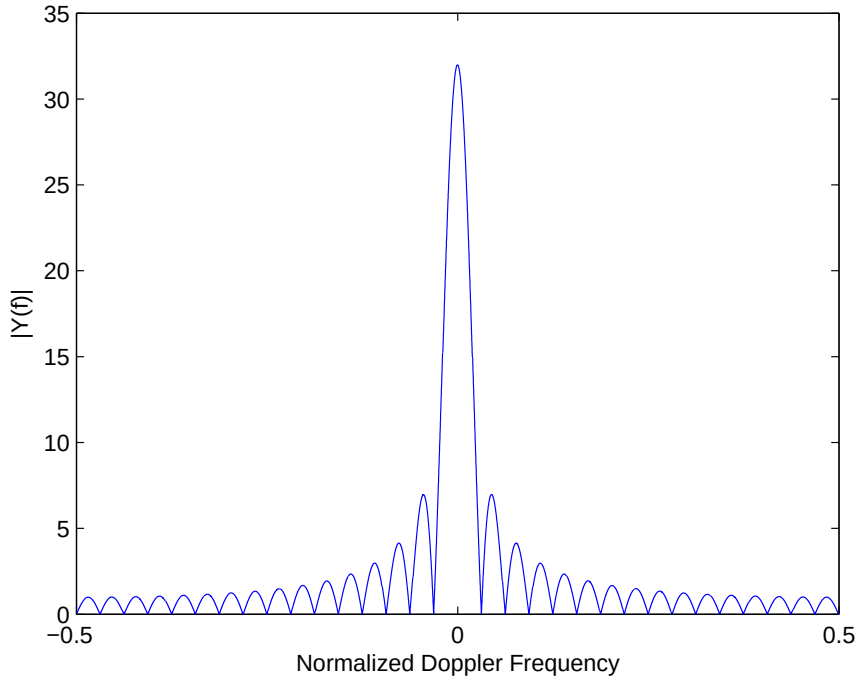

Figure 3.1: Magnitude of the Fourier transform of slow time received signal for a point target.

decrease the detection performance. Also, windowing causes an increase in the main lobe width, which decreases the accuracy of Doppler frequency estimation [3]. These effects of windowing can be seen in Figure 3.2, which is the Doppler spectrum of the same data in Figure 3.1, except that a Hamming window is applied.

The second problem that the waveform given by equation (3.4) causes is the fact that in practice this waveform is never observed. Since the frequency variable in this waveform is continuous, the discrete time Fourier transform (DTFT) of the slow time received signal is not computed. Instead of this, the discrete Fourier transform (DFT), which is the sampled version of the DTFT, of the slow time received signal is computed commonly [26]. The problem with computing the DFT is that, since the DFT is the sampled version of the DTFT, it is possible that this sampling process can miss the peak value of the DTFT. The DFT samples the peak value as in Figure 3.3 when the Doppler frequency of the target coincides

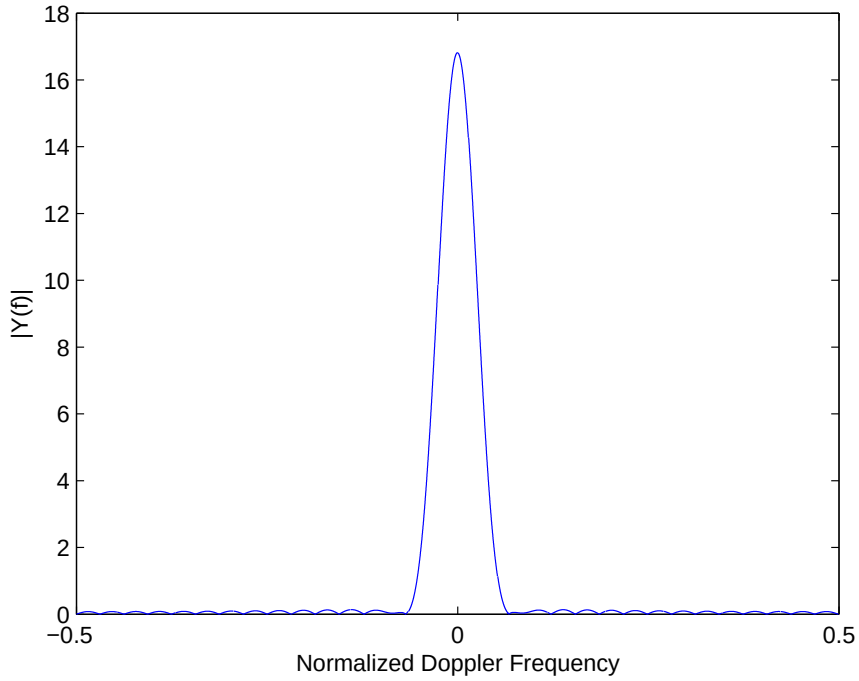

Figure 3.2: The magnitude of the Fourier transform of the windowed slow time received signal from a point target.

with the frequency of one of the DFT samples. However, when the Doppler frequency of the target does not coincide with one of the DFT sample frequencies, the expected peak value is missed. Especially, when the Doppler frequency of the target is exactly the halfway between two consecutive DFT sample frequencies, the smallest amplitudes are observed as in Figure 3.4. Since it is not always possible that the Doppler frequency of the target coincides with one of the DFT sample frequencies, most of the time the peak value is missed, which decreases the performance of the traditional CFAR algorithms. Also another problem is that there are commonly two samples with larger amplitudes than the others as in Figure 3.4, which makes it difficult to obtained a precise estimate of the target's Doppler frequency.

The most common solution to these problems is to increase the length of the DFT. In that way, the frequency range is sampled with more points and this decreases the possibility of missing the peak value [1]. The problem with this

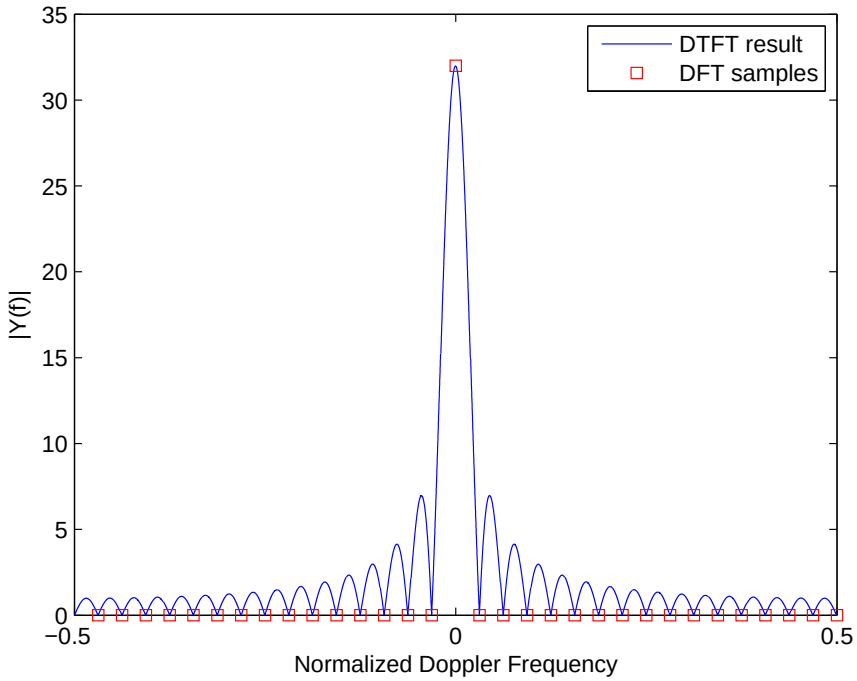

Figure 3.3: The magnitude of the DTFT of the slow time received signal from a point target and the DFT samples when the Doppler frequency of the target coincides with one of the DFT sample frequencies.

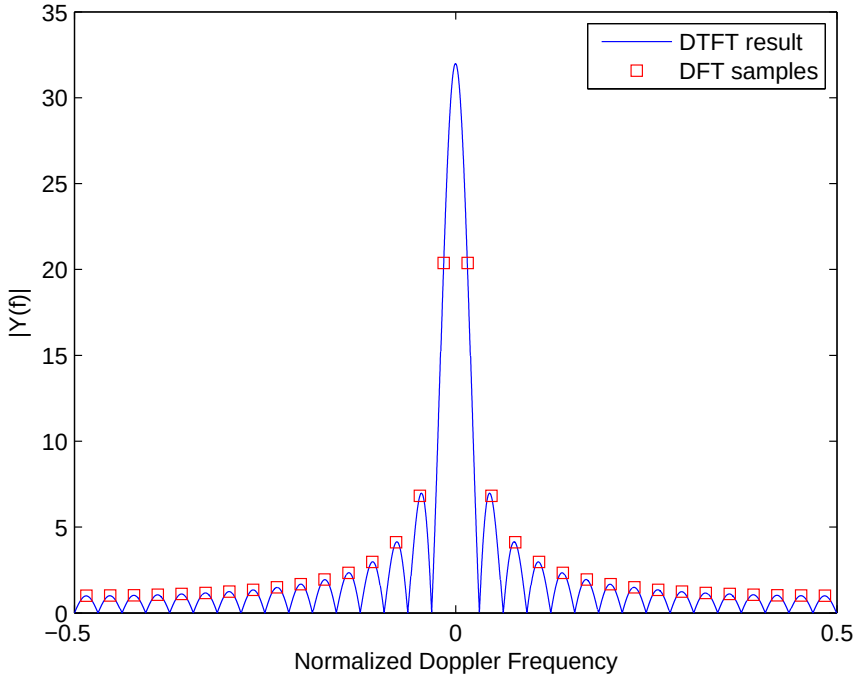

Figure 3.4: The magnitude of the DTFT of the slow time received signal from a point target and the DFT samples when the Doppler frequency of the target is halfway between the two consecutive DFT sample frequencies.

solution is that it increases the computational cost. Also, the number of cells in the detection matrix is increased, which means that the number of times that the CFAR algorithm is executed increases. Another solution is again windowing the slow time received signal. As explained above, windowing increases the width of the main lobe, which decreases the possibility of missing the peak value. However, as discussed before, windowing decreases the SNR; hence, the detection performance.

3.2 Optimal Solution for the Estimation of Target Doppler Frequency

The optimal solution for the estimation of target Doppler frequency is studied in this section. First, the optimal solution for the case of one target is introduced. Then, the optimal solution for multiple targets is derived. Finally, the optimal solution without the knowledge of the number of targets is proposed.

3.2.1 Optimal Solution for One Target

As studied before, the Fourier transform of the slow time ideal received signal for one point target is given by

$$Y(f-f_D) = A\frac{\sin[\pi(f-f_D)MT]}{\sin[\pi(f-f_D)T]}\, e^{-j\pi(M-1)(f-f_D)T}, \quad f \in [-PRF/2, +PRF/2), \tag{3.5}$$

where M is the number of pulses, PRF is the radar's pulse repetition frequency, T is the pulse repetition interval, and f_D is the Doppler shift caused by the velocity of the target.

The ideal signal in (3.5) is not what we observe after pulse Doppler processing in practice. Since the DFT is used instead of the DTFT, what we observe is the

sampled version of equation (3.5). The observed signal in the absence of noise can be expressed as

$$\mathbf{y}_{A,f_D}(i) = A\frac{\sin[\pi(f_i - f_D)MT]}{\sin[\pi(f_i - f_D)T]}e^{-j\pi(M-1)(f_i-f_D)T} \quad \text{for } i = 1, 2, 3, \ldots, M \ , \tag{3.6}$$

where $f_i = -PRF/2 + (i-1)(PRF/M)$.

Let $\mathbf{s}$ define the signal that would be observed in the absence of noise. In the case of one target, $\mathbf{s}$ is equal to $\mathbf{y}_{A,f_D}$. The noise is modeled as complex Gaussian noise with unit variance,

$$\mathbf{n} \sim \mathcal{CN}(\underline{0}, \sigma^2\mathbf{I}) \ , \tag{3.7}$$

and the observed signal in the presence of noise is the sum of the ideal signal and noise; that is,

$$\mathbf{r} \ = \ \mathbf{s} + \mathbf{n} \ . \tag{3.8}$$

In addition to noise, there are two unknown parameters in vector $\mathbf{r}$. These two parameters are A and f_D that are defined in equation (3.5). An optimal solution for estimating these parameters is the maximum likelihood (ML) solution [2]. The likelihood function in this case can be written as

$$L(\mathbf{r}) = \frac{\frac{1}{2\pi^M\sigma^{2M}}\exp\left\{-\sum_{i=1}^{M}\frac{|\mathbf{r}(i)-\mathbf{s}(i)|^2}{2\sigma^2}\right\}}{\frac{1}{2\pi^M\sigma^{2M}}\exp\left\{-\sum_{i=1}^{M}\frac{|\mathbf{r}(i)|^2}{2\sigma^2}\right\}} \ . \tag{3.9}$$

Then, after some manipulation, the log-likelihood function can be obtained as

$$\log L(\mathbf{r}) = k - \frac{1}{2\sigma^2}\left\{\sum_{i=1}^{M}|\mathbf{s}(i)|^2 - 2\sum_{i=1}^{M}Re\{\mathbf{s}^*(i)\mathbf{r}(i)\}\right\} \ , \tag{3.10}$$

where k represents a constant that does not depend on the unknown parameters.

The maximization of the log-likelihood function in equation (3.10) results in

$$\arg\max_{A,f_D} \ \left\{2\sum_{i=1}^{M}Re\{\mathbf{s}^*(i)\mathbf{r}(i)\} - \sum_{i=1}^{M}|\mathbf{s}(i)|^2\right\} \ . \tag{3.11}$$

Equation (3.11) finds the optimum values of A and f_D that maximize the log-likelihood function. The value of f_D calculated via this equation is the result of the optimal solution for estimating the Doppler frequency in the case of one target.

3.2.2 Optimal Solution for Multiple Targets

In the case of one target, signal $\mathbf{s}$, defined as the signal that would be observed in the absence of noise, is equal to $\mathbf{y}_{A,f_D}$ as discussed in Section 3.2.1. In equation (3.6), $\mathbf{y}_{A,f_D}$ is defined to be the observed signal from just one point target with amplitude A and whose velocity causes a Doppler shift of f_D. In the case of multiple, say k, targets, the definition of $\mathbf{s}$ needs to be generalized. Since the signals coming from the targets will have different amplitudes and different Doppler shifts, $\mathbf{s}$ can be written as

$$\mathbf{s} = \sum_{i=1}^{k} A_i \mathbf{y}_{f_{D_i}} \ , \tag{3.12}$$

where A_i and f_{D_i} are the amplitude and the Doppler shift of ith target, respectively.

The structure of the (log-)likelihood equations in (3.9)-(3.11) remains the same for the case of k targets except that $\mathbf{s}$ is changed as in equation (3.12). Then, the ML solution can be expressed as

$$\arg\max_{\mathbf{A},\mathbf{f}_D} \left\{ 2\sum_{i=1}^{M} Re\{\mathbf{s}^*(i)\mathbf{r}(i)\} - \sum_{i=1}^{M} |\mathbf{s}(i)|^2 \right\} \ . \tag{3.13}$$

The main difference of this equation from the one target case is that, in (3.13), the maximization is performed over two vectors $\mathbf{A}$ and $\mathbf{f}_D$, which are both k dimensional. For the one target case, the solution is the result of a 2 dimensional optimization problem but for the case of k targets the dimension of the optimization problem is $2k$. It is straightforward to observe that the complexity of the solution increases with the increasing number of targets.

3.2.3 Optimal Solution for Unknown Number of Targets

In the previous cases, the only unknown parameters are the Doppler shifts and the amplitudes of the target signals, since the number of targets is assumed to be

known. When the number of targets is unknown, another unknown parameter is introduced into the estimation problem and the optimization procedure should be performed accordingly. In this scenario, $\mathbf{s}$, the signal component in the absence of noise, should be indexed by the number of targets; that is,

$$\mathbf{s}_k = \sum_{i=1}^{k} A_i \mathbf{y}_{f_{D_i}} , \qquad k = 1, 2, \ldots, M . \tag{3.14}$$

Again the equations in (3.9)-(3.11) can be employed to obtain the ML solution:

$$\arg \max_{\mathbf{A}, \mathbf{f}_D, k} \left\{ 2 \sum_{i=1}^{M} Re\{\mathbf{s}_k^*(i)\mathbf{r}(i)\} - \sum_{i=1}^{M} |\mathbf{s}_k(i)|^2 \right\}, \tag{3.15}$$

which now includes the number of targets as another unknown parameter. Including a new variable increases the complexity of this optimization problem extremely, since the optimal parameter values need to be searched for all possible numbers of targets. In the case of one target, it was sufficient to solve an optimization problem with only 2 parameters. Increasing the number of targets increases the computational complexity in such a way that when there are k targets, $2k$ parameters needed to be optimized. But when the number of targets is unknown, the optimization problem must be solved for each possible number of targets. For example, when $M = 32$, first an optimization problem with 2 parameters, then with 4 parameters, then with 6 parameters must be solved. And this goes all the way up to 64 parameters. However instead of solving the optimization problem in equation (3.15) for each posible number of targets we can consider the largest possible number of targets for k and solve the optimization problem. Then among these k targets the ones with their amplitudes larger than a threshold can be selected as the detected targets. By doing this computational complexity of the optimal solution can be decreased and also the algorithm can avoid to match very weak targets to pure noise.

Since in practical applications, the number of targets is generally unknown and the number of pulses is generally high, such as 32, 64 or 128, the optimal solution is quite impractical to use due to its high computational complexity.

3.3 Suboptimal Solutions

Since the high computational complexity of the optimal solution makes it quite impractical, suboptimal solutions that are easier to implement are needed. Here two suboptimal solutions will be proposed. Both of these solutions use the fact that the waveform given by equation (3.6) is known except for some of its parameters. The first solution is very simple to implement and its complexity is very low. The second one is a more complex solution but its performance is supposed to be better and its complexity is still significantly lower than that of the optimal solution in the previous section.

3.3.1 Maximum Selection

As discussed before, the signal model of a point target in the Doppler domain, given by equation (3.4), is in the form of a sinc function. The nice property of this signal model is that it achieves its maximum value at the target's Doppler frequency as it can be seen in Figure 3.1. Based on this fact, it can be concluded that the Doppler cells with large amplitudes are more likely to be the ones that include a target. The maximum selection algorithm relies on this observation and results in the following simple two step algorithm.

1. Assume it is known that there are k targets.
2. Choose the k cells with the largest amplitudes to be the ones with the targets.

This is a technique with very low complexity. Of course, the tradeoff is that there are some weaknesses of this approach that needs extra attention. First of all, as studied in Section 3.1, the observed signal is not the same as the one in Figure 3.1, but a sampled version of it. When the Doppler frequency of

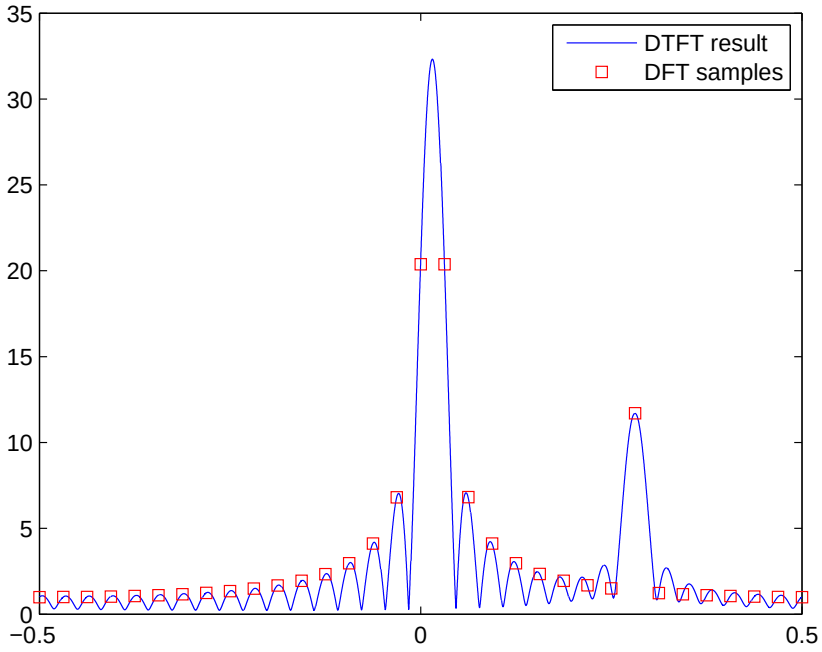

Figure 3.5: The magnitude of the DTFT of the slow time received signal from two point targets and the DFT samples.

the target does not coincide with one of the DFT sample frequencies, the peak value is not sampled. The worst possible scenario in this situation is that the Doppler frequency of the target is exactly the halfway between two consecutive DFT sample frequencies. But even in that case two sample frequencies with the largest amplitudes are very close to the actual Doppler frequency of the target as can be seen in Figure 3.4. The problem in such a situation is that lower values are observed, since the peak value is missed, and it is possible to miss these lower values especially at low SNRs.

Another problem with this approach is that when there are more than one target, a stronger target may block the detection of weaker targets. For example, in Figure (3.5), if it is known that there are two targets, two cells with the largest amplitudes are chosen and those two cells belong to the same target; hence the weaker target is missed.

3.3.2 Successive Cancelation

The successive cancelation technique uses the fact that, given A and f_D, the signal coming from a point target is completely known as it is given by equation (3.6). This approach obtains the unknown parameters for one target first, and using these parameters recreates the signal coming from that target. Then, it subtracts the recreated signal from the observed signal. The technique repeats this procedure until there are no more targets. The steps of the algorithm can be listed as follows:

1. Assume it is known that there are k targets in the same range bin.
2. Find A and f_D satisfying:

$$[\hat{A}\ \hat{f}_D] = \arg\min_{A,\, f_D} \ |\mathbf{r} - \mathbf{y}_{A,f_D}|, \qquad f_D \,\epsilon\, [-PRF/2, +PRF/2]\ . \tag{3.16}$$

3. Assume A and f_D are the magnitude and the Doppler frequency of a target.
4. Generate vector $\mathbf{y}_{\hat{A},\hat{f}_D}$ according to equation (3.6).
5. Subtract $\mathbf{y}_{\hat{A},\hat{f}_D}$ from $\mathbf{r}$ in equation (3.8).
6. Repeat these steps k times.

The second step of the algorithm is actually the same as the maximization of the likelihood function for the optimal solution for one target given by equation (3.11). So this algorithm uses the optimal solution for one target successively as long as there are no more remaining targets in the observed signal. The advantage of this approach is that its complexity is lower than the optimal solution. In this approach, when there are k targets, k different optimization problems with 2 parameters need to be solved. But as it is mentioned in Subsection 3.2.3, the optimal solution requires to solve M different optimization problems. The first of these optimization problems has 2 parameters, the second one has 4 parameters and this goes all the way up to $2M$ parameters.

3.3.3 Suboptimal Solutions with Unknown Number of Targets

The suboptimal solutions in the previous sections assume that the number of targets is known. However, in practical applications, it is not always possible to know the number of targets. To handle this problem, it is necessary to find a condition to stop the iterations.

For both suboptimal solutions, a threshold that satisfies a specific constant false alarm rate is required. In order to obtain such a threshold, the assumption of complex Gaussian noise with zero mean and unit variance, given by equation (3.7), will be used. Consider independent and identically distributed (iid) noise as

$$Z = X + iY \tag{3.17}$$

where both X and Y are Gaussian random variables with standard deviation σ. In this case, $|Z|$, which is equal to $\sqrt{X^2 + Y^2}$, is Rayleigh distributed with parameter σ:

$$|Z| \sim Rayleigh(\sigma) \tag{3.18}$$

For this distribution, the probability of false alarm can be defined as

$$P_{FA} = \int_{\gamma}^{\infty} \frac{r}{\sigma^2} \exp\left\{\frac{-r^2}{2\sigma^2}\right\} dr \ , \tag{3.19}$$

which can be further simplified as

$$P_{FA} = \exp\left\{\frac{-\gamma^2}{2\sigma^2}\right\} \ . \tag{3.20}$$

The assumption of unit variance, that is $\sigma = 1/\sqrt{2}$, simplifies P_{FA} to

$$P_{FA} = \exp\left\{-\gamma^2\right\} \ . \tag{3.21}$$

From equation (3.21), the threshold for a specified P_{FA} can be written as

$$\gamma = \sqrt{-\ln(P_{FA})} \ . \tag{3.22}$$

Using this threshold, the proposed suboptimal solutions can be used without knowing the number of targets. The algorithms for the suboptimal solutions for the cases of a known number of targets can be updated by using this threshold in the case of an unknown number of targets. Then, the algorithm for the maximum selection technique becomes

1. Check if there are any cells with amplitudes larger than γ.
2. Choose the cells with the amplitudes that are larger than γ to be the ones with the targets.

On the other hand, the algorithm for successive cancelation can be formulated as

1. Check if there are any cells with amplitudes larger than γ.
2. Find A and f_D satisfying:

$$[\hat{A}\ \hat{f}_D] = \arg\min_{A,\, f_D} \ |\mathbf{r} - \mathbf{y}_{A,f_D}|, \quad f_D \,\epsilon\, [-PRF/2, +PRF/2]\ . \tag{3.23}$$

3. Assume that $\hat{A}$ and $\hat{f}_D$ are the magnitude and the Doppler frequency of a target.
4. Generate the vector $\mathbf{y}_{\hat{A},\hat{f}_D}$ according to equation (3.6).
5. Subtract $\mathbf{y}_{\hat{A},\hat{f}_D}$ from $\mathbf{r}$ in equation (3.8).
6. Repeat these steps as long as there is a cell with an amplitude that is larger than γ.

Chapter 4

PERFORMANCE EVALUATION

In this chapter, detailed performance analysis of the methods described in Chapter 3 is presented. First, some useful definitions are given. Then, the performance of the proposed methods are investigated for various scenarios.

4.1 Definition of System Parameters

In order to make fair performance analysis of the proposed algorithms, the parameters that are used in the simulations must be defined properly. One of the most important parameters in these simulations is the target SNR. Throughout all the simulations, the target SNR is defined as

$$SNR = 10 \log \left\{ \frac{\sum_{i=1}^{i=M} |s(i)|^2}{\sigma^2} \right\} , \tag{4.1}$$

where $\mathbf{s}$ is the noiseless received signal from a target and σ is the standard variation of the complex Gaussian noise.

Another important parameter is related to the Doppler frequency bins of the target. As discussed before, the received signal in the Doppler domain is a vector of length M, where M is the number of pulses in the transmitted signal. Each of these Doppler frequency bins corresponds to one of the DFT sample frequencies. During the simulations it is assumed that a target belongs to the ith Doppler frequency bin if its Doppler frequency is between $f_i - f_s/2$ and $f_i + f_s/2$, where f_i is the frequency of the ith DFT sample and f_s is the frequency difference between two consecutive DFT samples.

Detection probabilities of the algorithms will be the key parameter to compare their performances with each other. We will accept a decision as a correct detection if a target in the ith Doppler frequency bin is detected exactly at the ith Doppler frequency bin. Otherwise, that decision will be assumed to be a false alarm. But this is different from the conventional definition of the probability of false alarm, which is commonly defined in the presence of background noise only.

As it is mentioned in the previous chapter, optimal solution and successive cancellation requires to solve an optimization problem. In the simulations particle swarm optimization (PSO), is used to solve the optimization problems. PSO is a widely used method for global optimization [27].

4.2 Simulation Scenarios

Five different scenarios are considered for the simulations. Each of these simulations is performed for the case of a transmitted signal with 32 pulses, which is a common number in pulse Doppler radar systems. In each simulation, there are three targets. Three targets at the same range may seem as a large number, but it is important to have more than one targets at the same range to test the algorithms in difficult scenarios. In first four scenarios, targets with the same

SNR are used, but their locations are different in each case. For the last scenario targets with different SNRs are used.

4.2.1 Scenario I

In this scenario, the three targets are placed at equal distances in the sense that the first target is at the 13th, the second one is at the 16th and the last one is at the 19th Doppler frequency bin. The distance of three frequency bins between the targets is important here. Because of the fact that the actual Doppler frequency of a target is most probably different from the DFT sample frequency corresponding to its Doppler frequency bin, the main lobe of the received signal from that target may extend to two neighbor Doppler frequency bins. In this situation, a three-bin distance is safe enough to distinguish the targets from each other.

First, performances of the algorithms are investigated under the assumption of a known number of targets. As can be observed from Figure 4.1, the performances of the optimal solution and successive cancelation is very close to each other at all SNR values, whereas the maximum selection algorithm performs worse than the others for all SNRs, even though its performance is closer to the other ones at high SNRs. In the case of a known number of targets, there is no need to investigate the probability of false alarm separately since it is simply equal to $1 - P_D$.

Next, the performances of the algorithms are compared for the case of an unknown number of targets. In this case, the following observations are important for fair a comparison. As explained in Chapter 3, the optimal solution in the case of an unknown number of targets does not use a specific probability of false alarm, whereas the successive cancelation and maximum selection need a probability of false alarm to determine when to stop the iterations. In order to

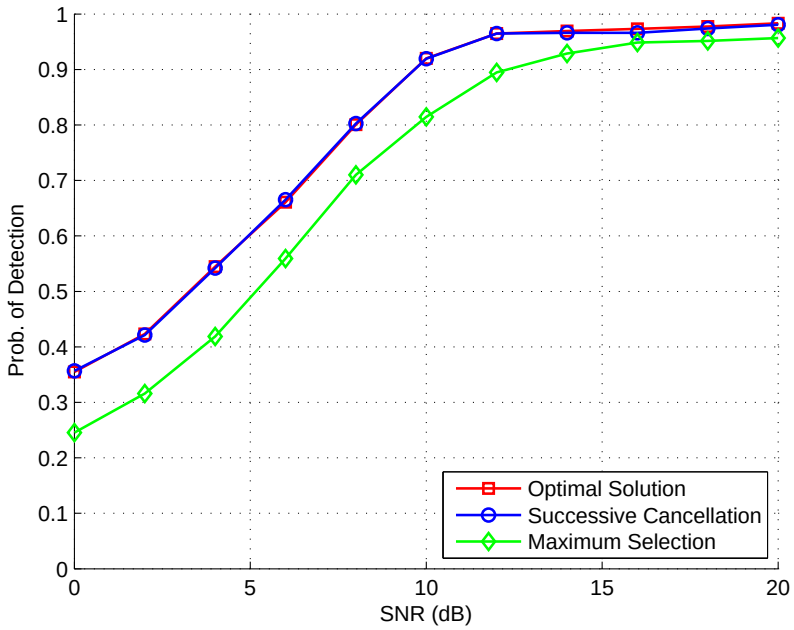

Figure 4.1: Probability of detection for optimal solution, successive cancelation and maximum selection with a known number of targets for scenario I.

make a fair comparison of these algorithms, the probability of false alarm observed from the simulations for the optimal solution will be found first, and then that probability of false alarm for different SNR values will be used as inputs for the successive cancelation and maximum selection algorithms.

For the case of an unknown number of targets, performance of the optimal solution can be seen in Figure 4.2. It is observed that at high SNR values the detection performance of the optimal solution is almost same as the case of a known number of targets. At low SNR values, it can be seen that the probability of detection is also higher than that in the case of a known number of targets; however, the probability of false alarm is also higher. In Figure 4.3, the probabilities of detection for each algorithm are illustrated. As discussed before, the probability of false alarm for each algorithm is chosen to be the same. In this case, the performances of the optimal solution and successive cancelation are almost the same at all SNR values. On the other hand, maximum selection

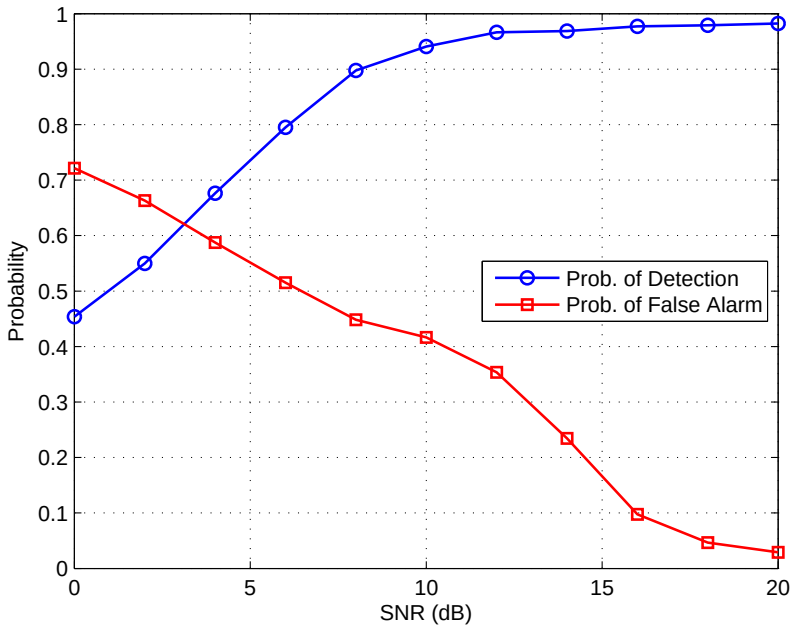

Figure 4.2: Probability of detection and false alarm for the optimal solution with an unknown number of targets for scenario I.

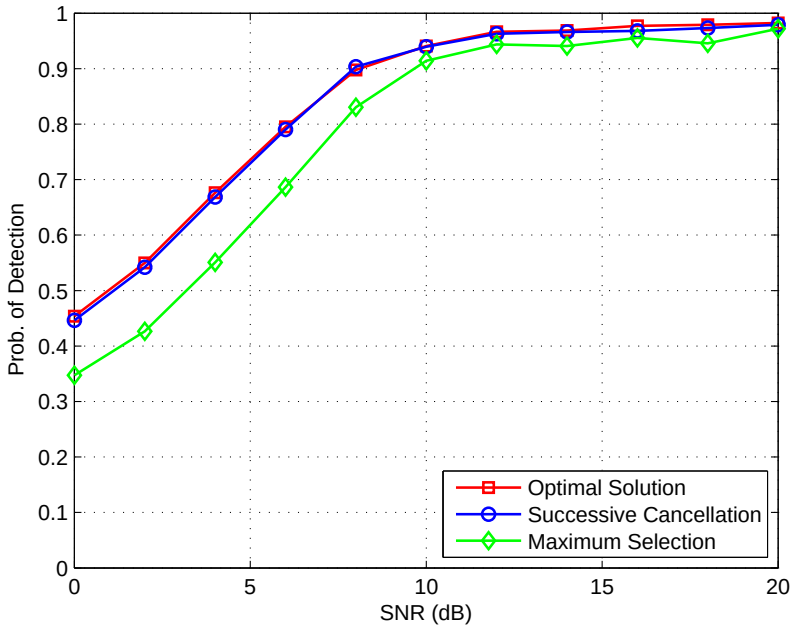

Figure 4.3: Probability of detection for the optimal solution, successive cancelation and maximum selection with an unknown number of targets for scenario I.

performs worse at low SNRs, but its performance gets closer to the other two algorithms as SNR increases.

4.2.2 Scenario II

In this scenario, all the three targets are again placed at an equal distance in the Doppler domain. However, this time they are closer to each other. The first target is at the 14th, the second one is at the 16th and the last one is at the 18th Doppler frequency bin. The distance of two frequency bins between the targets is critical. As explained before, the main lobe of the received signal from a target may extend to two neighbor Doppler frequency bins. In this situation, two bin distance makes it difficult to detect the targets successfully, because it is possible that two neighboring targets can increase the amplitude of the bin between them where there is no target.

First, the performances of the algorithms are investigated under the assumption of a known number of targets. As can be seen in Figure 4.4, the performances of the optimal solution and successive cancelation are very close to each other at all SNR values. However, unlike scenario I, successive cancelation performs a little worse than the optimal solution at high SNRs. The reason of this can be the iterative approach of the algorithm. Since it finds targets one by one, it is possible to make a wrong decision when the targets are very close to each other. Maximum selection performs worse than the others at all SNR values, and at high SNRs its performance is closer to the other algorithms.

For the case of an unknown number of targets, the performance of the optimal solution can be investigated in Figure 4.5, which reveals that the detection performance of the optimal solution is almost the same as the case of a known number of targets at high SNRs. At low SNRs, it can be seen that the probability of detection is also higher than the case of a known number of targets; however,

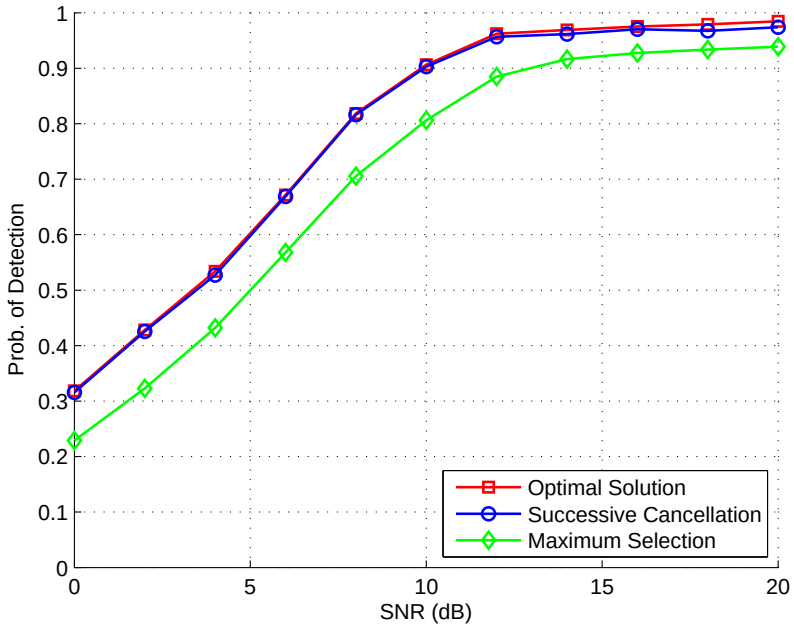

Figure 4.4: Probability of detection for the optimal solution, successive cancelation and maximum selection with a known number of targets for scenario II.

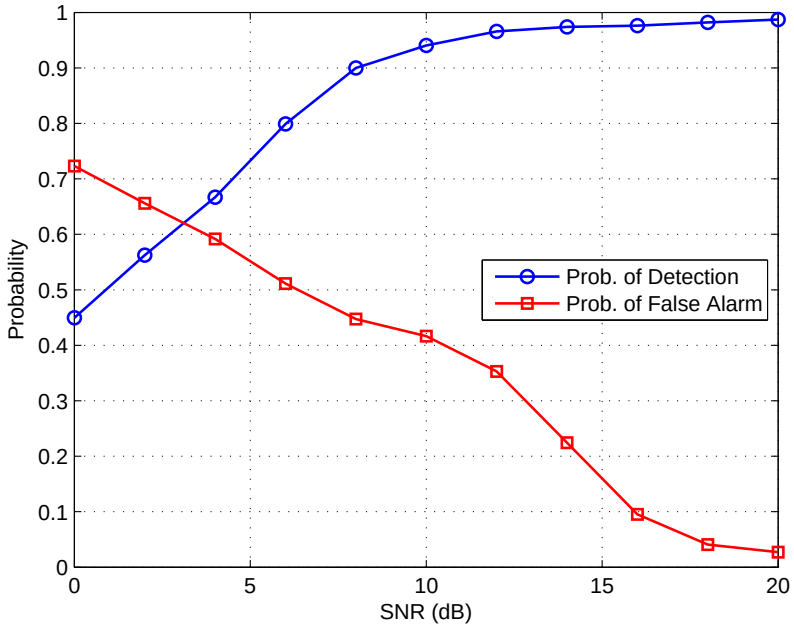

Figure 4.5: Probability of detection and false alarm for the optimal solution with an unknown number of targets for scenario II.

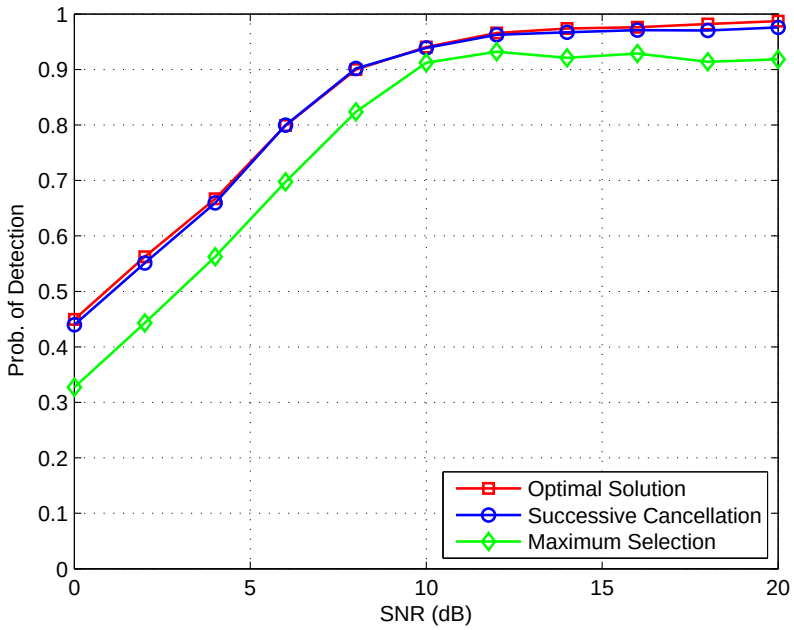

Figure 4.6: Probability of detection for the optimal solution, successive cancelation and maximum selection with an unknown number of targets for scenario II.

the probability of false alarm is also higher. In Figure 4.6, the probabilities of detection for each algorithm are given. As explained before, the probability of false alarm for each algorithm is chosen to be the same. In this case, the performances of the optimal solution and successive cancelation are almost the same at all SNR values, but at high SNRs the performance of successive cancelation is a little worse. As it is explained in the previous paragraph, this is because of the nature of the scenario. On the other hand, maximum selection performs the worst and its performance does not improve at all after an SNR of 10 dB.

4.2.3 Scenario III

Since estimating the Doppler frequency of close targets is a difficult task, it will be the most difficult scenario when two targets are at adjacent Doppler frequency bins. In this scenario, the first target is at the 14th, the second one is at the 16th and the last one is at the 17th Doppler frequency bin. The targets at the 16th

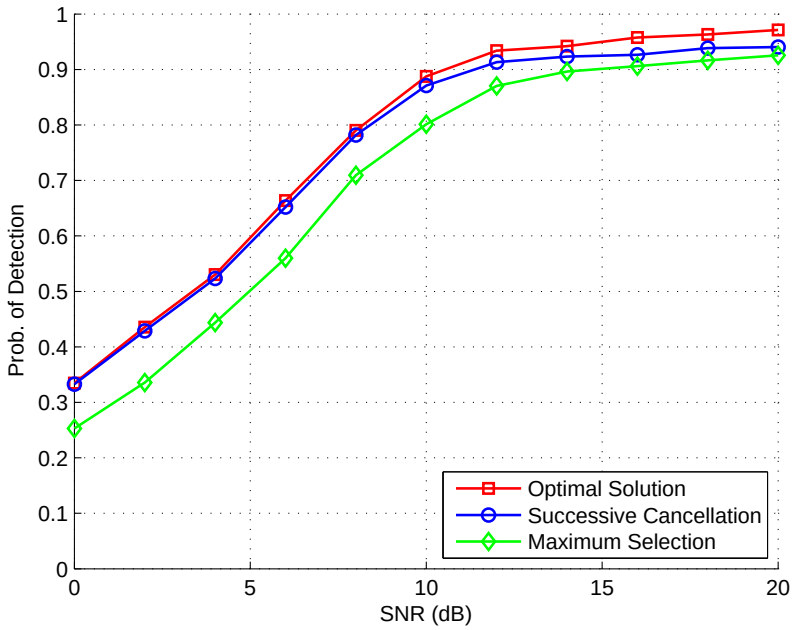

Figure 4.7: Probability of detection for the optimal solution, successive cancelation and maximum selection with a known number of targets for scenario III.

and the 17th bins make the detection challenging. Since they are very close to each other, it is possible that they can be detected as just one target and this can decrease the performance of the algorithms.

First, the performances of the algorithms are investigated under the assumption of a known number of targets. As can be seen in Figure 4.7, even the performance of the optimal solution is lower than the first two scenarios. This is because of the fact that it is a more difficult scenario as explained above. As in Scenario II, at high SNR values, successive cancelation performs a little worse than the optimal solution although their performances at low SNRs are very close to each other. The reason of this is the same as the reason explained in Scenario II. The iterative approach of successive cancelation can make mistakes when two targets are very close to each other. Maximum selection performs worse than the others at low SNR values but at high SNRs its performance gets closer to the other algorithms.

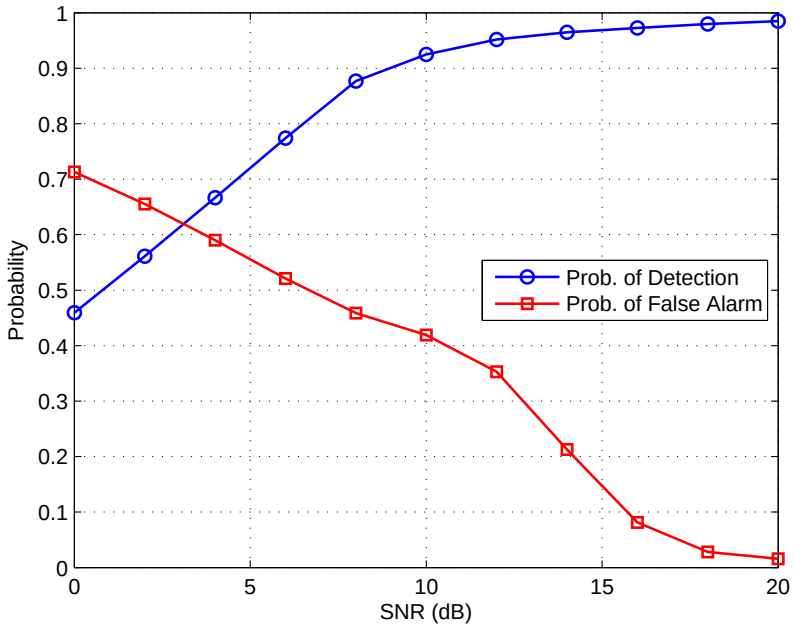

Figure 4.8: Probability of detection and false alarm for optimal solution with an unknown number of targets for scenario III.

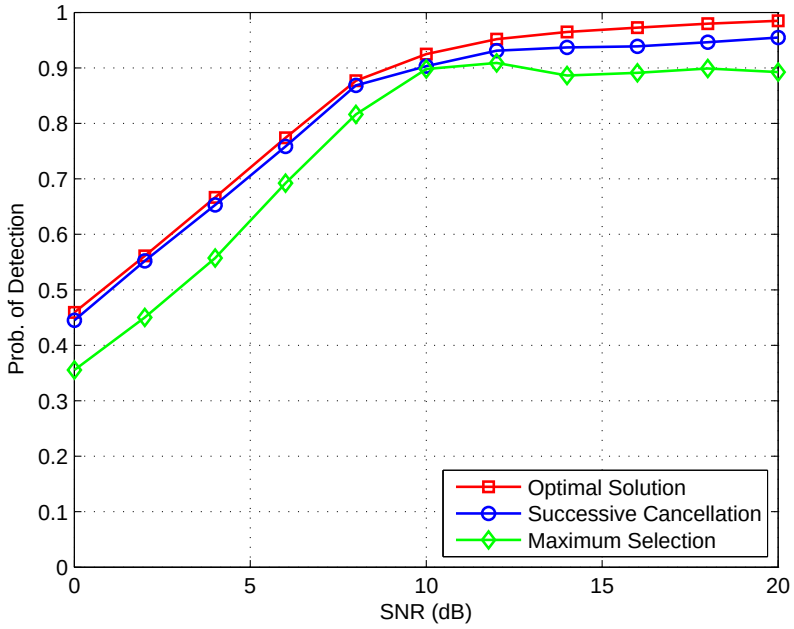

Figure 4.9: Probability of detection for optimal solution, successive cancelation and maximum selection with an unknown number of targets for scenario III.

For the case of an unknown number of targets, the performance of the optimal solution can be obtained as in Figure 4.8. It is observed that the detection performance of the optimal solution is a slightly better than the case of a known number of targets at high SNR values. Since in the case of a known number of targets, the algorithm was restricted to find just three targets whereas in the case of an unknown number of targets there is no such restriction, the probability of detecting the close targets is increased. However, this also increases the probability of false alarm. In Figure 4.9, the probability of detection for each algorithm is given. As explained before, the probability of false alarm for each algorithm is chosen to be the same. In this case, the performances of the optimal solution and successive cancelation are almost the same at all SNR values, but at high SNRs the performance of successive cancelation is slightly worse. As discussed in the previous paragraph, this is because of the nature of the scenario. On the other hand, maximum selection has the worst performance and it does not improve at all after an SNR of 10 dB.

4.2.4 Scenario IV

This is the final scenario in which all the target have the same SNR. This time, in the simulations, the targets are placed at random Doppler frequency bins for each trial. Also, each Doppler frequency bin is allowed to have one target at most.

First, the performances of the algorithms are investigated under the assumption of a known number of targets. As can be seen in Figure 4.10, the performances of the optimal solution and successive cancelation are very close to each other at all SNRs. However, the optimal solution performs slightly better at high SNRs. The reason of this is simply the same as that in scenarios II and III. Since the targets are placed at the Doppler frequency bins randomly, it is possible in some cases that there are very close targets, which decreases the performance

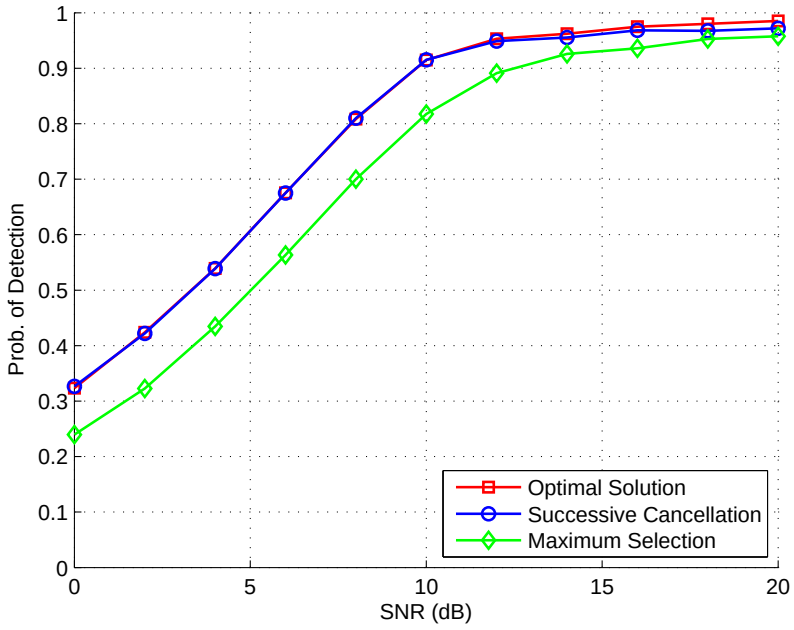

Figure 4.10: Probability of detection for optimal solution, successive cancelation and maximum selection with a known number of targets for scenario IV.

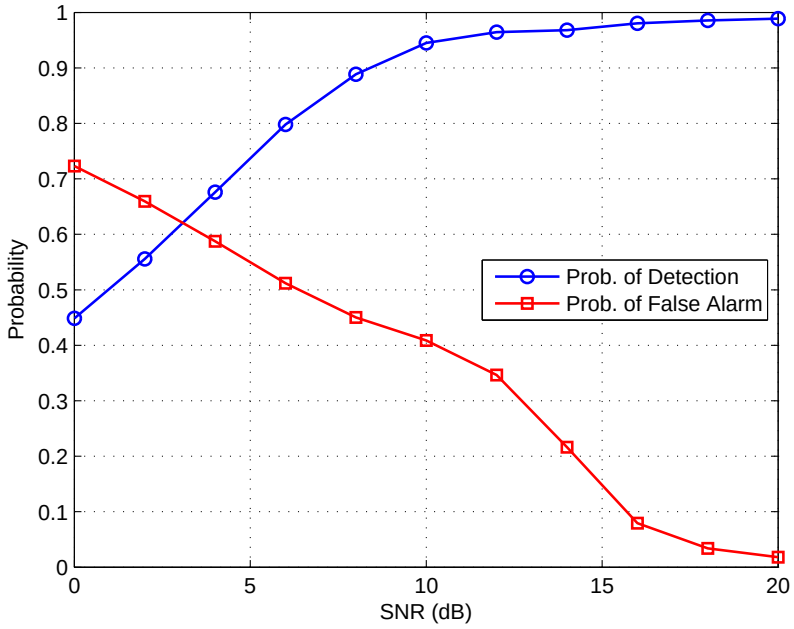

Figure 4.11: Probability of detection and false alarm for optimal solution with an unknown number of targets for scenario IV.

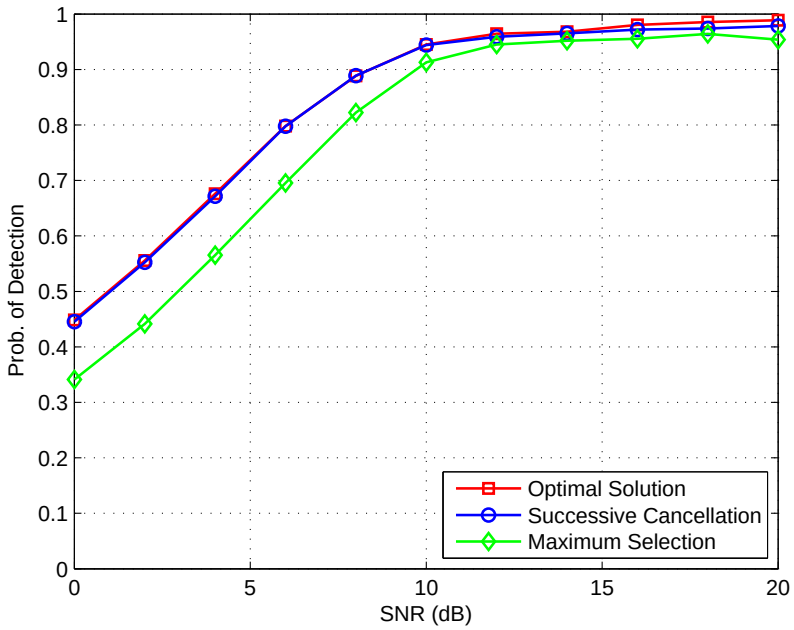

Figure 4.12: Probability of detection for optimal solution, successive cancelation and maximum selection with an unknown number of targets for scenario IV.

of successive cancelation. However, unlike scenario I, successive cancelation performs slightly worse than the optimal solution at high SNR values. The main reason of this is the iterative approach of the algorithm. Since it finds targets one by one, it is possible to make a wrong decision when the targets are very close to each other. Maximum selection performs worse than the others at all SNRs even though its performance is closer to the other algorithms at high SNRs.

For the case of an unknown number of targets, the performance of the optimal solution can be seen in Figure 4.11, which indicates that the detection performance of the optimal solution is almost same as that in the case of a known number of targets at high SNRs. At low SNRs, it can be observed that the probability of detection is also higher than that in the case of a known number of targets. However, the probability of false alarm is also higher. In Figure 4.12, the probability of detection for each algorithm is given. As explained before, the probability of false alarm for each algorithm is chosen to be the same. In this case, the performances of the optimal solution and successive cancelation are

almost the same at all SNR values, but at high SNRs the performance of successive cancelation is slightly worse. As explained in the previous paragraph, this is because of the nature of the scenario. On the other hand, maximum selection performs worse at low SNR values, but its performance gets closer to the other two algorithms as SNR increases.

4.2.5 Scenario V

In this scenario, all the three targets are placed at an equal distance again. The first target is at the 14th, the second one is at the 16th and the last one is at the 18th Doppler frequency bin. But this time their SNR values are not same. The SNR of the target at the 16th bin is 5 dB higher than the others. The Doppler frequency bins of the targets are as in scenario II. Although scenario II is a challenging one, it is simpler than this scenario since but since all the targets have the same SNR in scenario II. In this scenario, the target in the middle has the potential to shadow the other two targets.

Since the targets do not have the same SNR, plotting the performance of the algorithms is not straightforward. For this scenario, the x-axis of the figures corresponds to the SNR of the weaker targets. First, the performances of the algorithms are investigated under the assumption of a known number of targets. As can be observed from Figure 4.13, the performances of the optimal solution and successive cancelation are very close to each other at all SNR values. Maximum selection performs worse than the others at all SNRs, and its performance does not improve much at high SNRs, which is an expected problem with this algorithm. When the targets have different SNRs, the side lobes of the strongest target may be larger than the weaker targets, and since maximum selection chooses the bins with the largest amplitudes to be the ones with the targets, it can miss weaker targets.

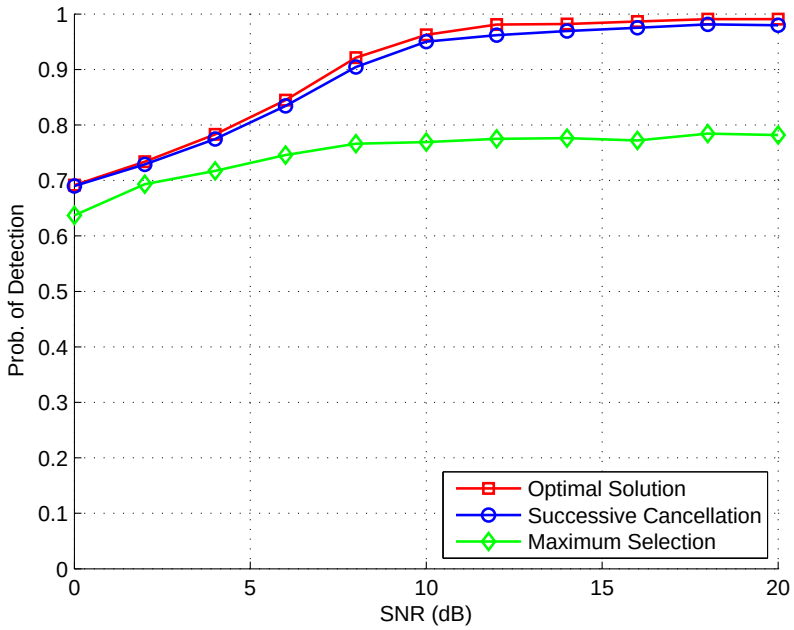

Figure 4.13: Probability of detection for optimal solution, successive cancelation and maximum selection with a known number of targets for scenario V.

For the case of an unknown number of targets, the performance of the optimal solution is illustrated in Figure 4.14. It is observed that at high SNR values the detection performance of the optimal solution is almost same as the case of a known number of targets. At low SNRs, it can be seen that the probability of detection is also higher than that in the case of a known number of targets, but the probability of false alarm is also higher. In Figure 4.15, the probabilities of detection are plotted for all the algorithms. As explained before, the probability of false alarm for each algorithm is chosen to be the same. In this case, the performances of the optimal solution and successive cancelation are almost the same at all SNR values. On the other hand, maximum selection performs the worst, but its performance is better than the case with a known number of targets.

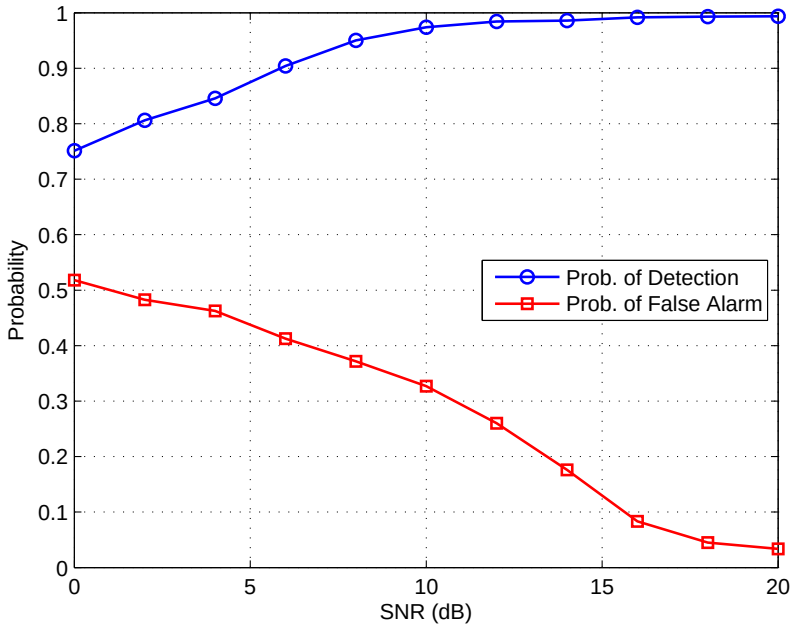

Figure 4.14: Probability of detection and false alarm for optimal solution with an unknown number of targets for scenario V.

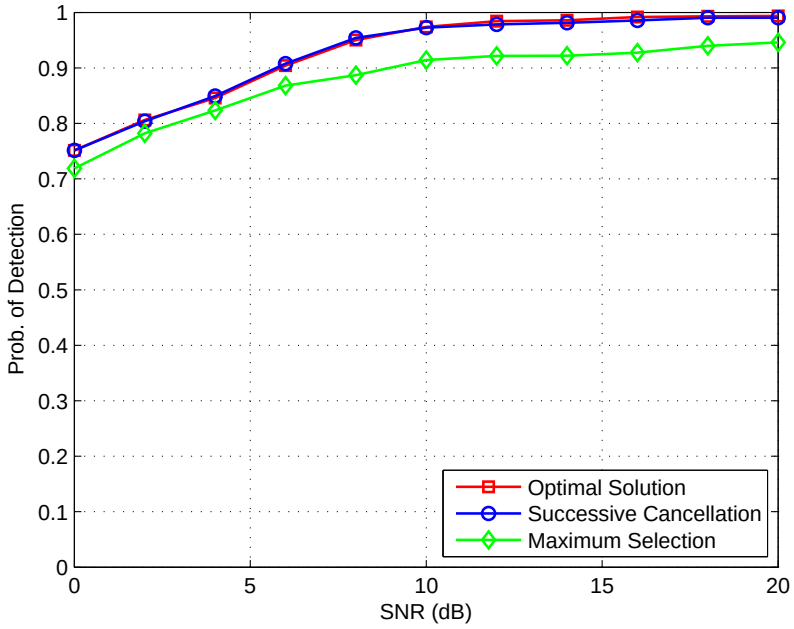

Figure 4.15: Probability of detection for optimal solution, successive cancelation and maximum selection with an unknown number of targets for scenario V.

Chapter 5

PERFORMANCE OF PROPOSED ALGORITHMS WITH REALISTIC TARGET MODELS

In the previous chapter, the detailed performance analysis of the proposed algorithms are provided for various cases of point targets. In this chapter, more realistic target models are presented, and the performances of the algorithms are investigated based on those realistic models.

5.1 Realistic Target Models

The algorithms presented so far are based on the fact that the observed signal model is known except for some of its parameters. However, this known model is the signal model for a point target. In real life applications, there are more complicated targets and the signal model for a point target cannot be observed

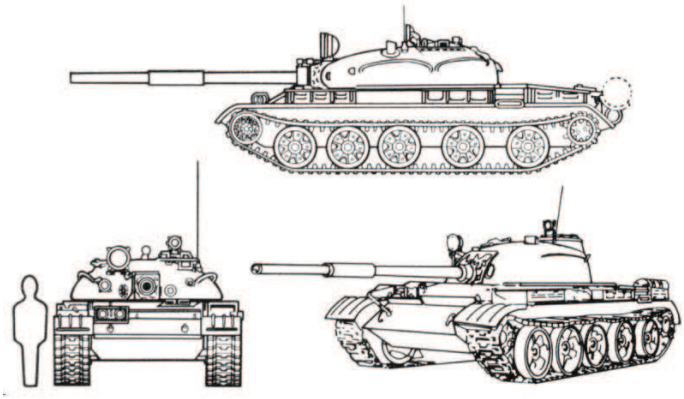

Figure 5.1: T-62 tank.

exactly. In order to investigate if this model can be used for realistic targets and, if not, what modifications can be done over this model, it is imperative to consider signals from real targets first.

Since radar applications have confidential importance, especially for military applications, it is very difficult to find real data. However, the in literature, there are some measurements for radar cross section areas which can help us model some realistic target models. Based on these measurements, three different real targets are modeled.

The first model is a Russian T-62 tank with a length of 6.63m, width of 3.52m, height of 2.4m and weight of 40, which is illustrated in Figure 5.1. In [28], radar cross section measurements for this target were performed with a monopulsed radar at 95 GHz. During the measurements, the tank was placed on a rotating platform and there was a distance of 95 m between the tank and the radar.

In order to model this tank and the other targets, it is first assumed that the targets are rectangular. Since the edges and the corners have the greatest cross section areas, the average value of the cross section area is assigned to the edges, the corners and the mid-point of the target, which make a total of 9 points. Finally, the small cross section values are assigned to 60 random points in the

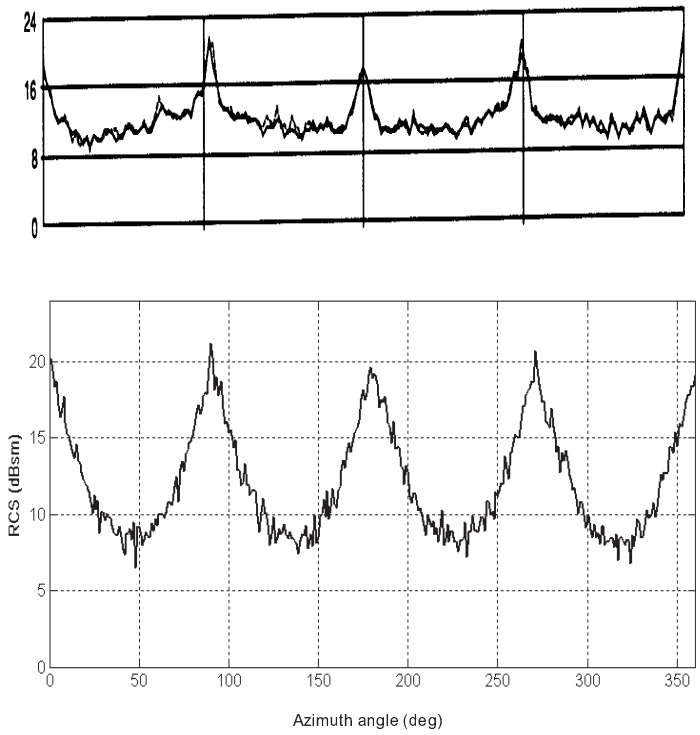

Figure 5.2: a) Measurement of radar cross section area values for the T-62 tank. b) Radar cross section area values of the model for the T-62 tank.

rectangular area. Radar cross section changes with the angle of view. Until now, the effect of this angle has not been defined in this model. In order to incorporate that effect, radar cross section values corresponding to some angles are chosen from the measurements and these values are matched to a polynomial function. In this way, a function representing all the angles is obtained. In the final step, the cross section values for all the 69 points are added, and this is multiplied with the function value of the degree at which the tank is supposed to reside. This gives a very realistic model as it can be seen in Figure 5.2.

The second target model is a French VAB armored vehicle with a length of 5.98m, width of 2.49m, height of 2.06m and weight of 13 tons, which is shown in Figure 5.3. For this target, two different measurements were performed in [29]. The first one was at 89 GHz with the real target and the second one was done at

890 GHz with a 1/10 model that corresponds to 89 GHz for the real size. Both measurements gave similar results and our model yielded close results to both measurements as it can be seen in Figure 5.4.

Figure 5.3: VAB armored vehicle.

The third model is another Russian tank, T-72, with a length of 6.67m, width of 3.59m and height of 2.19m, which is shown in Figure 5.5. For this target two different measurements were done in [30]. First one was at 359 GHz with a 1/35 model and the second one was done at 160 GHz with a 1/16 model which corresponds to 10 GHz in real size. Both measurements gave similar results and our model gave results close to both measurements as can be seen in Figure 5.6.

5.2 Optimal Solution and Successive Cancelation with Real Targets

Idea behind the maximum selection algorithm was simply to choose the cells with the largest amplitudes to be the ones with a target. Changing from point targets to real targets actually does not change anything for this algorithm. Therefore, in this chapter, only the optimal solution and successive cancelation are studied.

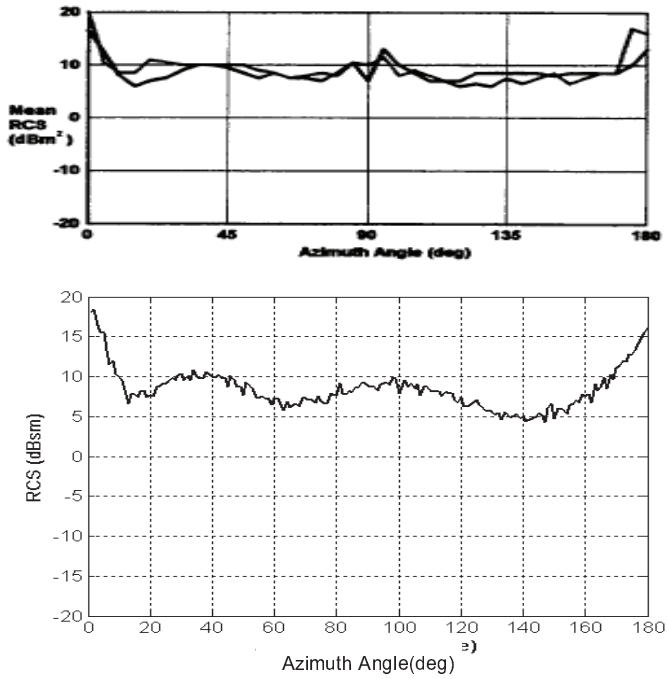

Figure 5.4: a) Measurement of radar cross section area values for VAB armored vehicle. b) Radar cross section area values of the model for VAB armored vehicle.

Originally, the signal model that the optimal solution and successive cancelation uses is for a point target. In order to see how well this model matches the signals coming real targets, the signals from the realistic target models are considered here in the absence of noise. Since there is noise, performance of the algorithms will not be presented as in Chapter 4 with figures of probability of detection vs SNR. Instead to check the performance of the algorithms, expected received signals will be recreated using the parameters estimated by these algorithms and these signals will be compared with the signal coming from the real targets.

First, the signals are produced for each target model such that there is just one target at the same range bin. As studied in the previous chapters, when there is one target, the optimal solution and successive cancelation perform almost the same. Therefore, for this case, only one estimated signal for each target is given. As observed from Figures 5.7, 5.8 and 5.9, the estimated signals are not exactly

Figure 5.5: T-72 tank.

the same as the received signal, but they are still very close to each other, and, most importantly, the Doppler frequencies of the targets are estimated correctly.

Since the waveform used in the algorithms are the waveforms of a point target, it is expected to see that estimated signals are not exactly the same as the received signals obtained from the realistic target models, even when there is no noise at all. However, the signals are quite similar and the estimation of the Doppler frequencies of the targets can be performed accurately.

Next, instead of one target, three targets for each model is placed at the same range bin with different velocities (Doppler frequencies). First, the optimal solution is obtained. As can be seen in Figures 5.10, 5.11 and 5.12, the Doppler frequency estimation is generally accurate. The Doppler frequencies of only one target for both T-62 and T-72 are estimated with an error of one Doppler frequency bin only. The reason of this error can be the usage of a point target signal model. But since the Doppler frequencies of the other targets are estimated correctly, it is most probably because of the fact that the specific target's Doppler frequency is very close to the halfway between two adjacent Doppler frequency bins, which causes the algorithm to make a mistake. But in practice this small error is not so important because during tracking Kalman filter will fix it.

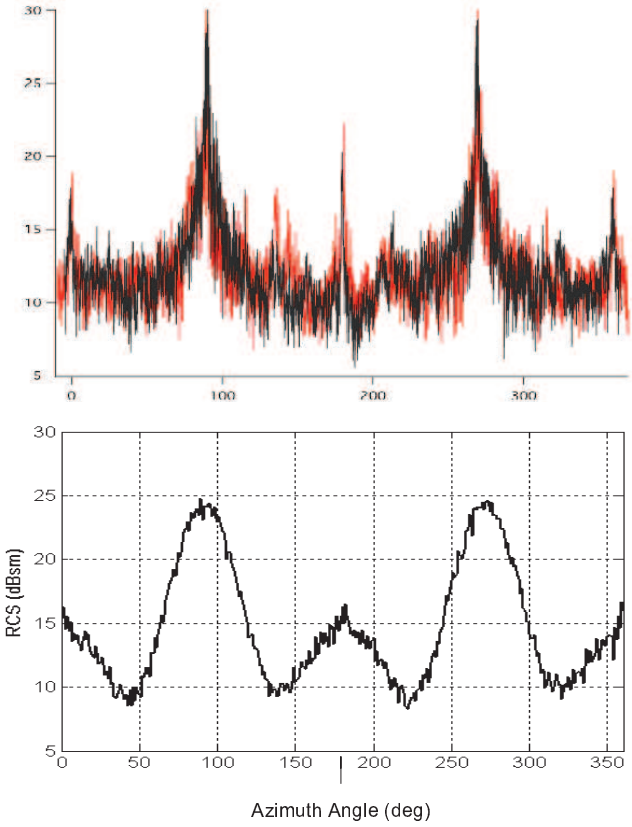

Figure 5.6: a) Measurement of radar cross section area values for the T-72 tank. b) Radar cross section area values of the model for the T-62 tank.

After the optimal solution, successive cancelation is performed on the same received signals. As can be observed from Figures 5.13, 5.14 and 5.15, the results are very similar to those obtained by using the optimal solution. Again for T-62 and T-72, the same Doppler frequencies of the targets are estimated with an error of one Doppler frequency bin.

These results show that, in the absence of noise, the point target model can be used to estimate the Doppler frequencies of real targets as well, even though the received signals cannot be estimated exactly by using this model. In other words, the Doppler frequencies of the realistic targets are estimated successfully for most of the time. Therefore, it is concluded that the proposed algorithms can also be used for realistic scenarios.

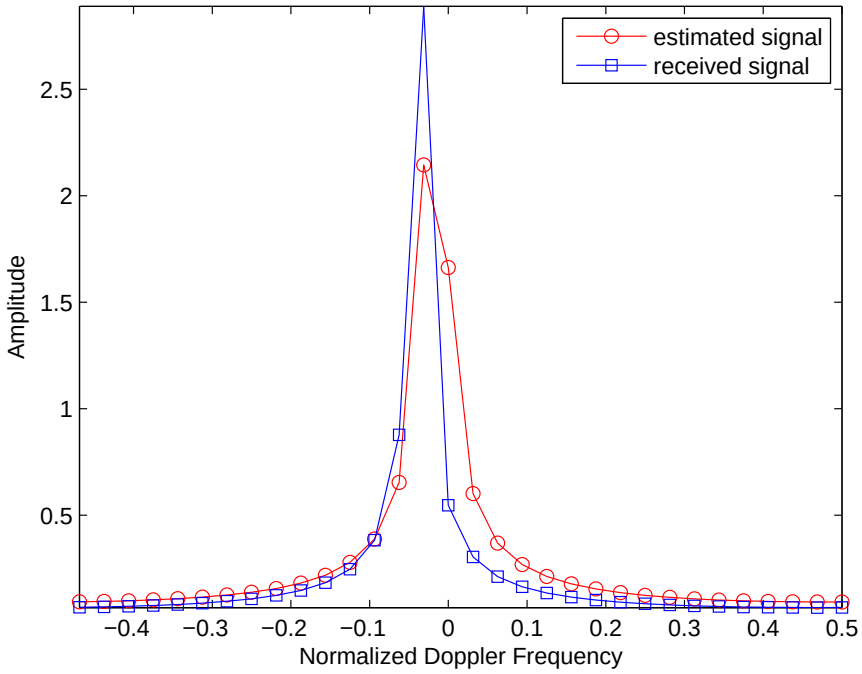

Figure 5.7: Received signal from one T-62 tank and estimated signal found by using the optimal solution or successive cancelation.

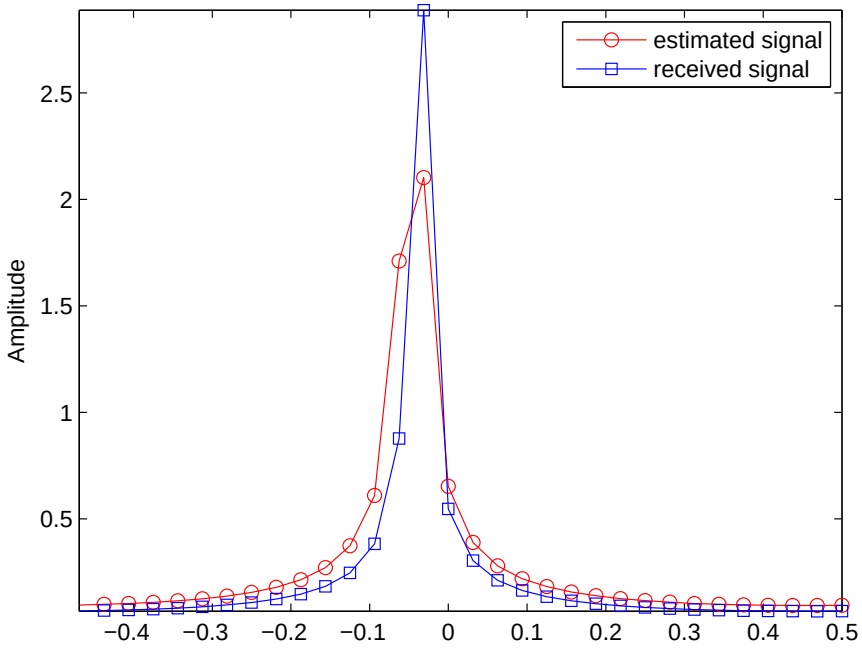

Figure 5.8: Received signal from one T-72 tank and estimated signal found by using the optimal solution or successive cancelation.

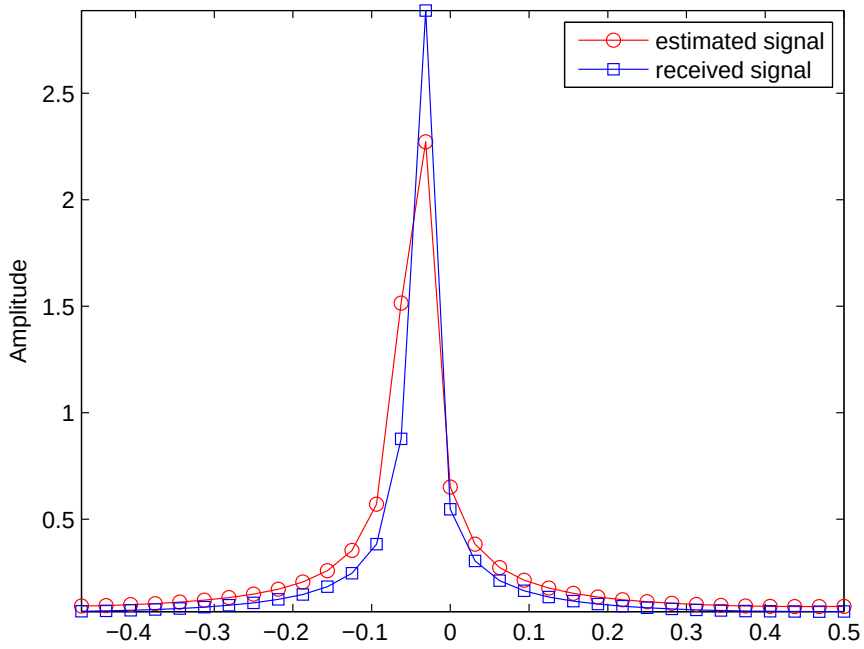

Figure 5.9: Received signal from one VAB armored vehicle and estimated signal found by using the optimal solution or successive cancelation.

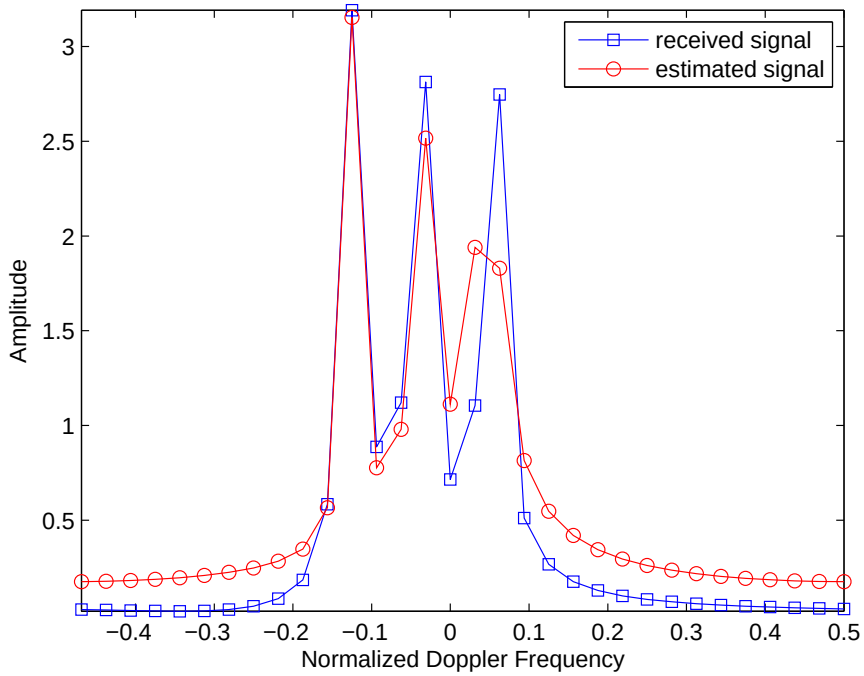

Figure 5.10: Received signal from three T-62 tanks and estimated signal found by using the optimal solution.

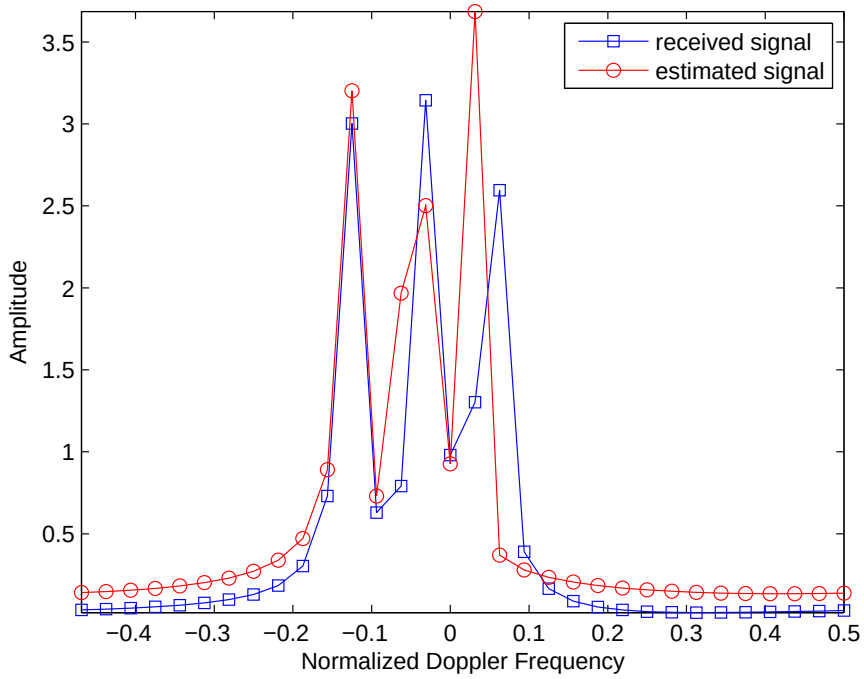

Figure 5.11: Received signal from three T-72 tanks and estimated signal found by using the optimal solution.

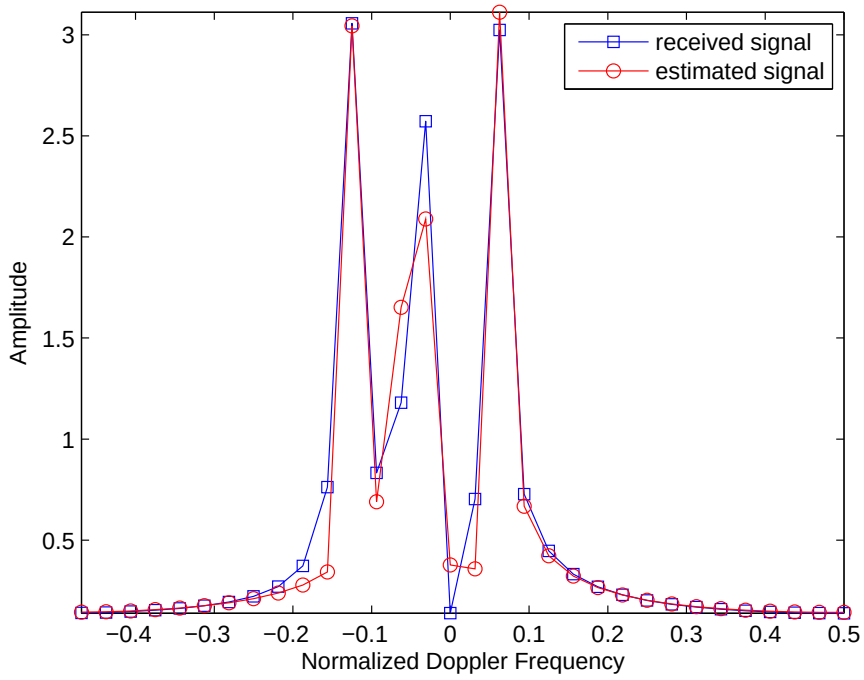

Figure 5.12: Received signal from three VAB armored Vehicles and Estimated Signal Found by Using the optimal solution.

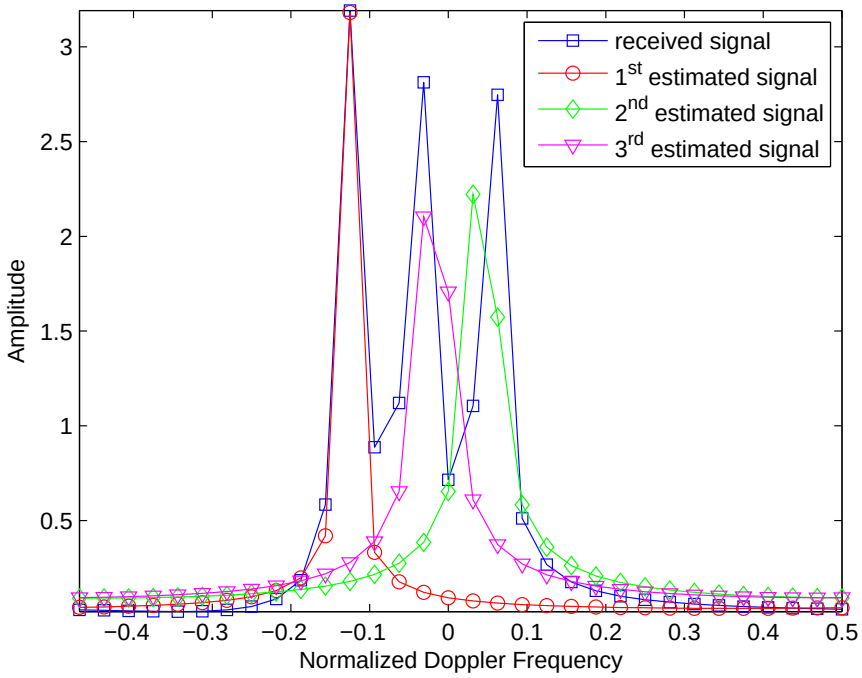

Figure 5.13: Received signal from three T-62 tanks and estimated signal found by using successive cancelation.

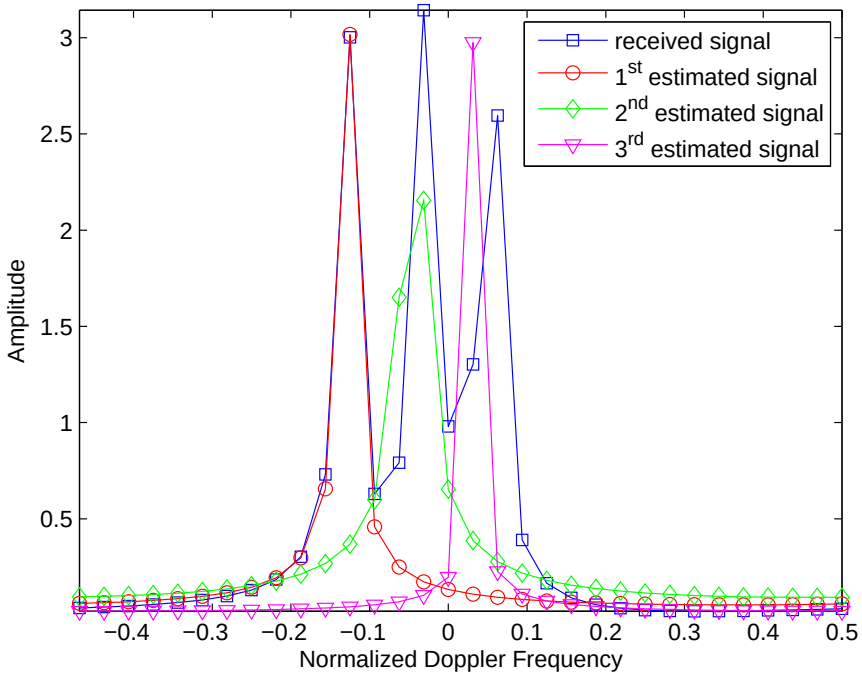

Figure 5.14: Received signal from three T-72 tanks and estimated signal found by using successive cancelation.

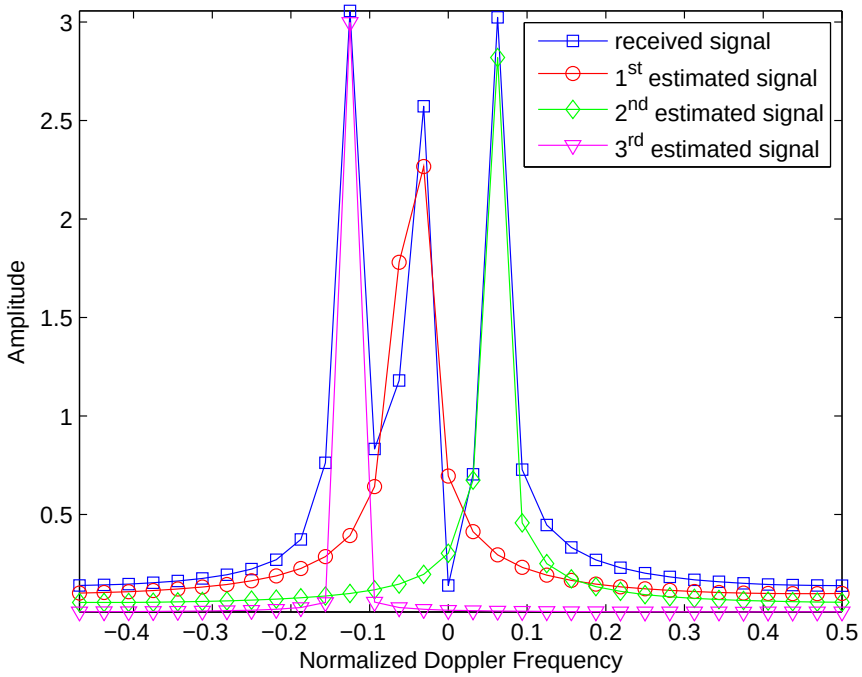

Figure 5.15: Received signal from three VAB armored vehicles and estimated signal found by using successive cancelation.

Chapter 6

CONCLUSIONS AND FUTURE WORK

In this thesis, new algorithms have been proposed for the estimation of the Doppler frequencies of targets in pulse Doppler radar systems. The main idea behind the algorithms is that since the waveform structure of a point target in the Doppler domain is known, it can be used to make more precise estimation of its Doppler frequency. First, the optimal solution which is the maximum likelihood (ML) estimator, has been derived. However, especially in the case of an unknown number of targets, the computational complexity of this solution is very high. Therefore, two suboptimal solutions with reasonable complexities have been proposed. The first one is successive cancelation, which is an iterative algorithm. In each iteration, a target that minimizes a cost function is specified, and the signal coming from that target is recreated. This recreated signal is subtracted from the received signal. In each iteration, these steps are repeated until there are no more targets left. The second suboptimal solution is the maximum selection algorithm, which uses the fact that the waveform of a point target in the Doppler domain achieves its maximum at the target's Doppler frequency;

hence, the algorithm chooses the Doppler bins with the largest amplitudes to be the ones with a target.

Several simulations have been performed to show that maximum selection performs worse than the optimal solution and successive cancelation at low SNRs. But at high SNR values, its performance gets closer to the other algorithms. However, since its computational complexity is very low, it can be an appropriate choice in some applications. On the other hand, successive cancelation provides a more complex solution but its performance is very close to the optimal solution at all SNR values. Also, it has been observed that successive cancelation can be used for real targets even though it uses the waveform of a point target.

Future work will be focused on improving the performance of the successive cancelation algorithm for real targets. Since there are no closed form expressions for the waveforms of real targets, it is more suitable to use the waveform of a point target with some additional parameters. Successive cancelation can also be used to perform Doppler estimation with higher resolution. The Doppler resolution of CFAR algorithms is limited with the number of pulses transmitted, whereas successive cancelation can estimate any number in the range as the Doppler frequency of a target. Furthermore, effects of ground clutter on this algorithm will be analyzed and some possible updates to the algorithm will be offered in order to perform better in the presence of clutter.

Bibliography

[1] M. A. Richards, *Fundamentals of Radar Signal Processing.* McGraw-Hill, 2005.

[2] H. V. Poor, *An Introduction to Signal Detection and Estimation.* New York: Springer-Verlag, 1994.

[3] F. J. Harris, "On the use of windows for harmonic analysis with the discrete fourier transform," *Proceedings of the IEEE*, vol. 68, no. 1, pp. 51–83, Jan. 1978.

[4] S. M. Kay, *Fundamentals of Statistical Signal Processing, vol. 2: Detection Theory.* Printice Hall, 1998.

[5] G. W. Stimson, *Introduction to Airborne Radar.* SciTech Publishing, 1998.

[6] C. E. Cook and M. Bernfeld, *Radar Signals An Introduction to Theory and Application.* London: Artech House, 1993.

[7] A. W. Rihaczek, *Principles of High Resolution Radar.* Boston: Artech House, 1996.

[8] N. Levanon and E. Mozeson, *Radar Signals.* New York: Wiley, 2004.

[9] R. Nitzberg, "Composite CFAR techniques," *Conference Record of The Twenty-Seventh Asilomar Conference on Signals, Systems and Computers*, vol. 2, pp. 1133–1137, 1993.

[10] S. Watts, "Cell-averaging CFAR gain in spatially correlated k-distributed clutter," *IEE Proceedings - Radar, Sonar and Navigation*, vol. 143, pp. 321–327, 1996.

[11] H. Rohling, "Radar CFAR thresholding in clutter and multiple target situations," *IEEE Transactions on Aerospace and Electronic Systems*, vol. AES-19, pp. 608–621, July 1983.

[12] M. Shor and N. Levanon, "Performances of order statistics CFAR," *IEEE Transactions on Aerospace and Electronic Systems*, vol. 27, pp. 214–224, March 1991.

[13] B. C. Armstrong and H. D. Griffiths, "CFAR detection of fluctuating targets in spatially correlated k-distributed clutter," *IEE Proc. Radar and Signal Processing*, vol. 138, pp. 139–152, April 1991.

[14] R. Srinivasan, "Simulation of CFAR detection algorithms for arbitrary clutter distributions," *IEE Proceedings - Radar, Sonar and Navigation*, vol. 147, pp. 31–40, Feb 2000.

[15] P. P. Gandhi and A. S. Kassam, "Analysis of CFAR processors in homogeneous background," *IEEE Transactions on Aeorospace and Electronics Systems*, vol. AES-24, no. 4, pp. 427–445, 1988.

[16] C. M. Wong and C. H. Chang, "CA-CFAR in weibull background," *2nd International Conference on Microwave and Millimeter Wave Technology*, pp. 691–694, 2000.

[17] E. Conte, M. Longo, and M. Lop, "Performance analysis of CA-CFAR in the presence of compound gaussian clutter," *Electronic Letters*, vol. 24, no. 13, pp. 782–783, 1988.

[18] I. Ozgunes, P. P. Gandhi, and A. S. Kassam, "A variably trimmed mean CFAR radar detector," *IEEE Transactions on Aeorospace and Electronics Systems*, vol. AES-28, no. 4, pp. 1002–1014, 1992.

[19] Y. He, X. Meng, and Y. Peng, "Performance of a new CFAR detector based on trimmed mean," *Proc. IEEE International Conference on Systems, Man, and Cybernetics*, vol. 1, pp. 702–706, Oct. 1996.

[20] M. B. E. Mashade, "Detection performance of the trimmed-mean CFAR processor with noncoherent integration," *IEE Proceedings - Radar, Sonar and Navigation*, vol. 142, pp. 18–24, Feb 1995.

[21] T. T. V. Cao, "A CFAR thresholding approach based on test cell statistics," *IEE Proceedings - Radar, Sonar and Navigation*, pp. 349–354, 2004.

[22] S. Blake, "OS-CFAR theory for multiple targets and nonuniform clutter," *IEEE Transactions on Aeorospace and Electronics Systems*, vol. AES-24, no. 6, pp. 785–790, 1988.

[23] N. B. Pulsone and R. S. Raghavan, "Analysis of an adaptive CFAR detector in non-gaussian interference," *IEEE Transactions on Aeorospace and Electronics Systems*, vol. 35, no. 3, pp. 903–916, July 1999.

[24] E. Conte, A. D. Maio, and G. Ricci, "Adaptive CFAR detection in compound-gaussian clutter with circulant covariance matrix," *IEEE Signal Processing Letters*, vol. 7, no. 3, pp. 63–65, March 2000.

[25] S. D. Himonas and M. Barkat, "Adaptive CFAR detection in partially correlated clutter," *IEE Proc. Radar and Signal Processing*, vol. 137, no. 5, pp. 387–394, Oct. 1990.

[26] S. M. Kay, *Modern Spectral Estimation*. Englewood Cliffs, NJ: Printice Hall, 1988.

[27] D. Bratton and J. Kennedy, "Defining a standard for particle swarm optimization," *IEEE Swarm Intelligence Symposium*, 2007.

[28] G. H. Goldman, "Point-scatterer model for a soviet t-62 tank at 95 ghz," *Army Research Laboratory*, pp. 1–32, Apr. 1995.

[29] D. Bird, "Target RCS modeling," *Radar Conference*, pp. 74–79, Mar. 1994.

[30] T. M. Goyette, J. C. Dickinson, C. Beaudoin, A. J. Gatesman, R. Giles, J. Waldman, and W. E. Nixon, "Acquisition of uhf and x-band ISAR imagery using 1/35th scale-models," *Proc. SPIE*, vol. 5808, Jun. 2005.